Front. Med. 2021, 15(5): 657–678
https://doi.org/10.1007/s11684-021-0829-6

REVIEW

Primary cilia in hard tissue development and diseases

Sijin Li[1], Han Zhang[2], Yao Sun (✉)[2]

[1]Department of Orthodontics, School & Hospital of Stomatology, Tongji University, Shanghai Engineering Research Center of Tooth Restoration and Regeneration, Shanghai 200072, China; [2]Department of Implantology, School & Hospital of Stomatology, Tongji University, Shanghai Engineering Research Center of Tooth Restoration and Regeneration, Shanghai 200072, China

Abstract **Bone and teeth are hard tissues. Hard tissue diseases have a serious effect on human survival and quality of life. Primary cilia are protrusions on the surfaces of cells. As antennas, they are distributed on the membrane surfaces of almost all mammalian cell types and participate in the development of organs and the maintenance of homeostasis. Mutations in cilium-related genes result in a variety of developmental and even lethal diseases. Patients with multiple ciliary gene mutations present overt changes in the skeletal system, suggesting that primary cilia are involved in hard tissue development and reconstruction. Furthermore, primary cilia act as sensors of external stimuli and regulate bone homeostasis. Specifically, substances are trafficked through primary cilia by intraflagellar transport, which affects key signaling pathways during hard tissue development. In this review, we summarize the roles of primary cilia in long bone development and remodeling from two perspectives: primary cilia signaling and sensory mechanisms. In addition, the cilium-related diseases of hard tissue and the manifestations of mutant cilia in the skeleton and teeth are described. We believe that all the findings will help with the intervention and treatment of related hard tissue genetic diseases.**

Keywords primary cilia; bone; mechanical sensing; hard tissue; cilium-related bone disease; tooth

Introduction

In vertebrates, bone is the architectural framework of the body structure and is critical for supporting physiologic loading and protecting internal organs. At the embryonic stage, bone is differentiated from the mesoderm and formed through intramembranous ossification or endochondral ossification [1,2]. Bone is renewed continuously throughout life to maintain its strength, maintain mineral homeostasis, and repair microdamage during bone remodeling [3]. Bone modeling and remodeling, which are both regulated by various physiological and mechanical factors, require the cooperation of osteoblasts and osteoclasts that direct the formation of new bone and the resorption of old bone, respectively [2,4].

In the skeletal system, the cell types involved in development and homeostasis regulation mainly include osteoprogenitor cells, chondrocytes, osteoblasts, osteocytes derived from mesenchymal stem cells (MSCs), and osteoclasts derived from hematopoietic stem cells [5]. At sites where long bones are formed via endochondral ossification, MSCs aggregate and differentiate into osteoprogenitor cells, which differentiate into chondroblasts and chondrocytes. Chondrocytes proliferate and form a hyaline cartilage framework and release alkaline phosphatase (ALP). This event is followed by hypertrophy and chondrocyte apoptosis. Dead chondrocytes create a barren matrix into which osteoprogenitors are recruited to derive osteoblasts [2]. Osteoblasts localize on bone matrix surfaces, synthesize and secrete bone matrix, and initiate matrix mineralization. Osteocytes are osteoblasts that are surrounded by matrix and live within lacunae. Osteoclasts absorb mineralized bone and participate in bone remodeling and healing [2,4]. In postnatal bone homeostasis regulation, a group of cells, which are defined as multipotent stem cells, act as the sources of bone healing or regeneration. These stem cells can be isolated from bone marrow, periosteum, skeletal muscle, fat, and umbilical cord blood and differentiate into specialized cells to function in remodeling, intramembranous ossification, or endochondral ossification [6].

Emerging evidence indicates the importance of primary cilia in bone development and cell function. Since primary cilia were first discovered on chondrocytes in 1967 [7], an

Received June 14, 2020; accepted October 13, 2020
Correspondence: Yao Sun, yaosun@tongji.edu.cn

increasing number of studies have focused on exploring their roles in chondrocyte biology, specifically endocytosis, infiltration, and apoptosis [8,9]. Further experiments found that primary cilia also exist in other cell types of the skeletal system, such as MSCs [10], MC3T3-E1 osteoblastic cells, MLO-Y4 osteocyte-like cells [11,12], and calvarial osteoblasts and osteocytes [11,13], and play important roles in bone development and remodeling. However, the existence of primary cilia on osteoclasts has yet to be proven [14].

Cilia are categorized into motile and primary cilia [15]. Primary cilia are present on the surfaces of almost all cell types in mammals, whereas motile cilia are found on respiratory epithelia and sperm flagella. Primary cilia appear like tiny antennas that protrude from the cell surface [16]. First named by Sergei Sorokin in 1968 [17], primary cilia have been considered as vestigial structures of no importance. However, increasing evidence suggests that primary cilia are functional organelles that not only can detect chemical or mechanical signals in the extracellular environment [18] but can also regulate cell mitosis [19] and signal transduction [20].

Primary cilia consist of the cilia axoneme, basal body, transition zone, and cilia membrane (Fig. 1). The axoneme is the main part of primary cilia and is composed of a ring of nine microtubule doublets. In contrast to the "9 + 2" motile cilia in respiratory epithelia or sperm flagella, primary cilia lack a central pair and other attachments, such as molecular motors and axonemal dyneins. Thus, primary cilia are nonmotile [21]. Cilia axonemes extend directly from a basal body that sits beneath the cell surface. This basal body consists of "9 + 0" microtubule triplets and is derived from the mother centriole; thus, the presence of primary cilia can inhibit the cell cycle [22]. Cilia microtubules have dynamic instability [23], and α-tubulin is acetylated to maintain microtubule stability [24]. Knocking out the mother centrosome localization protein *Nde1* elongates cilia; this effect then delays the cell cycle and disrupts cell growth [25,26]. A special structure called the "transition zone" is assembled at the junction of the axoneme and basal body, which is called the "cilia gate," and regulates the amount and speed of specific protein exchange between the cilia and the cell body, thereby controlling the strength of signal transduction [27]. For example, transmembrane protein 107 (TMEM107) is enriched in this region, and its mutation decreases the number of cilia [28]. A cilia axoneme is surrounded by a specialized membrane containing a set of specific receptors and channels, some of which are different from those contained by the cell membrane. This membrane is considered as the most important part of primary cilia because it serves as a receptor that senses external signals [29].

All ciliary proteins are synthesized in the cytosol and transported to cilia via intraflagellar transport (IFT), which is an evolutionarily conserved process that is required for axonemal growth and cilia maintenance [30,31]. IFT proteins form 2 complexes, complex A (IFT-A) and complex B (IFT-B). IFT-A components connect cargo to dynein-2 motors and carry it in the retrograde tip to the base direction, whereas IFT-B components bind proteins with kinesin-2 motors and carry them from the base to the tip in the anterograde direction [16,32,33]. Some ciliary proteins, including polycystin-1 (PC-1) and polycystin-2 (PC-2), smoothened (Smo), suppressor of fused (SuFu), and transcription factor glioma (Gli), are important components of signaling pathways, such as Hedgehog (Hh), Wnt, and PDGFRα [14,29,34]. The deficiency of primary cilia leads to abnormal Hh signaling and profound ectopic Wnt signaling [20]. In addition, multiple receptors and ion channels present on the primary cilia perceive signals, such as mechanical, light, chemical, and electronic field stimuli, from the surrounding environment. Cilia transduce these signals through various proteins and signaling pathways into cells [16,35]. Proteins with abnormal morphology or other defects cause reduced mechanical or biochemical susceptibility, which leads to abnormal signaling pathways [36]. However, the details of signal transduction into coordinated cellular responses by cilia remain elusive.

Primary cilia signaling in bone development

Cilia deficiency leads to ectopic signal transduction and skeletal system deformation [34,37]. Multiple signaling pathways associated with primary cilia have important effects on bone development and homeostasis. These pathways include Hh, Wnt, Notch, bone morphogenetic protein (BMP), PDGFR, and TGF (Fig. 2).

Hh

Hh signaling is one of the major pathways that regulates osteogenesis, embryonic bone development, and postembryonic bone homeostasis. Indian Hh (Ihh) regulates cartilage maturation during endochondral ossification, and Sonic Hh (Shh) regulates the patterning of the forming skeleton. Mice with the *Ihh* mutation have short statures and short, narrow ribs [38]. Day and Yang found that Hh signaling is greatly increased in all the bone tissues in mice with a single mutation in *Ptch1*, leading to the proliferation of cells especially in the perichondrium and articular cartilage [39]. The signaling component proteins Smo, SuFu, and Gli reside in cilia and are transported via IFT [34]. When Hh signaling is activated, Shh binds to the ligand receptor Ptc1 and releases Smo, which then moves to the cilium tip under facilitation by IFT-B and suppresses SuFu. This effect, in turn, releases the SuFu inhibition of

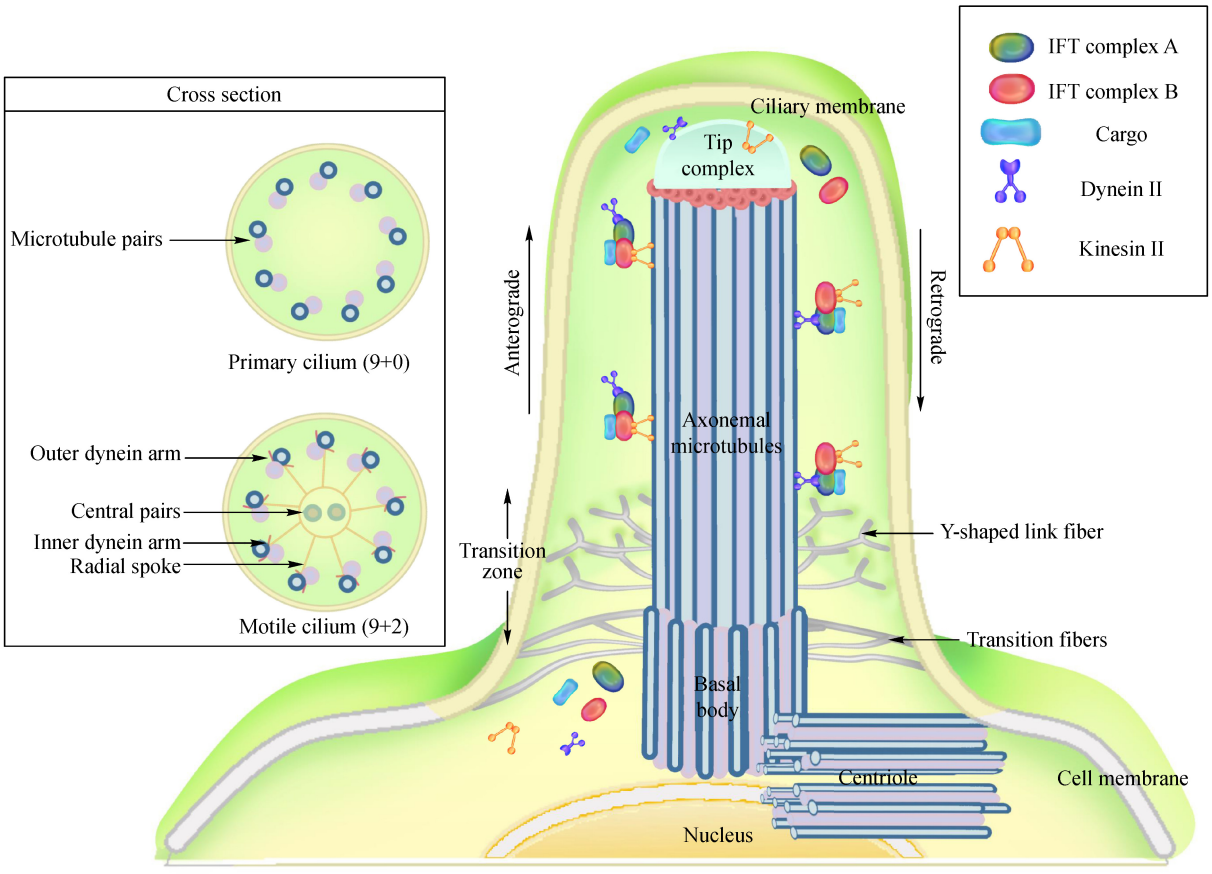

Fig. 1 Scheme of a fully assembled primary cilium and ciliary base structures. Primary cilia are composed of ciliated axonemal microtubules, basal bodies, transition zones, and ciliary membranes. Axonemal microtubules form the main part of primary cilia. The transition zone comprises Y-shaped linker proteins, ciliary necklace membrane proteins, and distal and subdistal appendages and acts as a diffusion barrier for ciliary proteins. Cilia are assembled and maintained through a bidirectional transportation system called IFT, which is mediated by IFT complexes and molecular motors that move along axonemal microtubules. IFT particles move with their cargo via the action of molecular motors kinesin 2 (anterograde trafficking) and cytoplasmic dynein 1b/2 (retrograde trafficking).

Gli and activates Gli to form Gli2A and Gli3A, which are transported to the nucleus and activate the expression of downstream target genes [20,39,40].

The loss of the Hh signaling pathway when cilia are missing leads to various skeletal deformities [31]. Some mutations in ciliary proteins block the response of Hh ligands, and other mutations block the activation of ligand-independent pathways [34]. Ihh and Shh disturbances can be seen in the endochondral ossification of *Ift88* conditional knockout (cKO) mice [41]. *Prx1-cre;Ift88*$^{fl/n}$ mutant mice exhibit severe polydactyly, and Gli1 expression is nearly abolished at E11.5. All *prx1-cre;Ift88*$^{fl/n}$ and *prx1-cre;Kif3a*$^{fl/n}$ mutants show a dramatic reduction in the overall length of skeletal elements and accelerated hypertrophic differentiation [41]. *Osterix-cre;Ift80* mice present osteopenia and defective osteoblast differentiation [31]. Silencing IFT80 causes cilia loss or shortens cilia length, leading to the loss of Hh signaling; a decrement in Gli2; and the suppression of the expression of osteoblastic marker genes, including runt-related transcription factor (*RUNX2*), *OCN*, *BMP2*, and *ALP*, thus resulting in the inhibition of ALP activity and cell mineralization. The expression of these genes can be rescued by the over-expression of Gli2 or the application of a Smo antagonist, indicating that IFT80 regulates bone differentiation and mineralization via Gli2 pathways, as well as osteoblastic marker genes [31].

Wnt

The canonical Wnt/β-catenin pathway promotes cell cycle and differentiation, whereas the noncanonical Wnt pathway regulates cell polarity and migration [42]. Wnt/β-catenin signaling acts in the Ihh pathway and downstream of Osx, regulating the whole osteogenic process and bone formation through intramembranous and endochondral

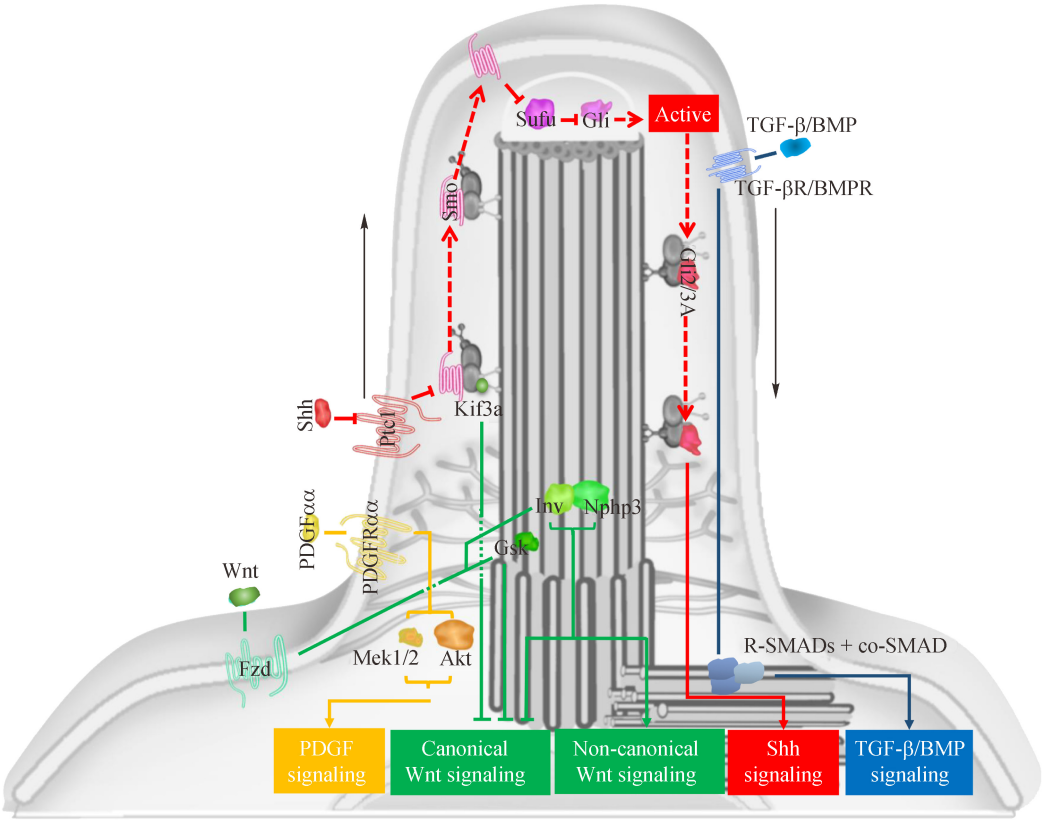

Fig. 2 Primary cilium-related signaling pathways in bone development. A variety of primary cilia signals, such as Sonic Hh, Wnt, PDGFR, and TGF-β, have important effects on bone development and homeostasis.

ossification [39,43]. Primary cilia attenuate the canonical Wnt signaling pathway by sequestrating β-catenin and preventing it from entering the nucleus, thus restricting the activation of downstream Wnt target genes [44]. Ciliotherapy with lithium chloride increases the length of primary cilia on MSCs; this effect leads to an increase in β-catenin localization to the nucleus [45]. Wnt components, such as Inversin, Fat4, and glycogen synthase kinase-3β (GSK-3β), are located in primary cilia [32]. GSK, inversin, and Kif3a [46] negatively regulate canonical Wnt/β-catenin. The ciliary protein NPHP3 inhibits canonical Wnt but activates noncanonical Wnt by binding with inversin [32,47]. After treatment with Ift88 siRNA or the Rho kinase inhibitor Y27632 to inhibit the formation of actin stress fibers, cilia length and number are reduced; these effects have been proven to affect MSC response to Wnt3a. The level of nuclear active β-catenin, the activation of the canonical Wnt pathway, and the proportion of cells entering the cell cycle all increased [36,48].

Platelet-derived growth factors

Platelet-derived growth factors (PDGFs) are growth factors that promote cell proliferation and migration. PDGF molecules bind to specific cell surface receptors, namely, PDGFRs, which are receptor tyrosine kinases that control a series of cellular processes, including osteogenic proliferation, cell survival, and endoplasmic reticulum (ER)–Golgi transport regulation; the latter function is the key to collagen secretion during skull development [49–52]. PDGFRα is located on the surfaces of primary cilia in fibroblasts during growth arrest [53]. PDGFRα expression is upregulated during ciliogenesis, and the expression and ligand-mediated activation of its receptor are blocked in *Ift88*$^{-/-}$ and *Ift172*$^{-/-}$ mouse embryonic fibroblasts (MEFs) [53,54]. Primary cilia contain the signaling machinery required for the pathway from PDGFRαα activation to Mek1/2 through Ras–Raf, controlling cell growth and proliferation [53]. PDGFRα regulates Akt phosphorylation through PDGFRα activation. The deletion of *Ift20* downregulates the transcription and translation of PDGFRα, thus suppressing PDGF–Akt signaling, resulting in decreased osteogenic proliferation and increased cell death rate [52].

TGF-β/BMP

The TGF-β superfamily is a large regulatory peptide that includes the model transforming growth factor-β family, BMP, and other families. TGF-β and BMP receptors are

located in primary cilia. Primary cilia mediate cell proliferation, differentiation, and migration by adjusting the output of canonical and noncanonical TGF-β signals and balancing the output of TGF-β/BMP signals [55,56]. In addition, the disruption of BMPs leads to embryonic lethality, limb patterning abnormalities, and cartilage condensation loss [57]. In the fracture model constructed with $Col2\alpha1^{cre}IFT80^{f/f}$ mice, the activation of the TGF-β signaling pathway is impaired, which leads to the interruption of cartilage callus formation and reduction in vascularization [58]. In smokers, the disruption of TGF-β signaling in MSCs under the mediation of cigarette smoke extract impairs endochondral ossification and delays fracture healing [59]. The elimination of primary cilia via transfection with IFT88 siRNA can block the activation of the BMP–Smad1/5/8 signal induced by pulsed electronic fields (PEMFs) and inhibit the increase in osteoblast differentiation and maturation [60]. The TGF-β1-mediated activation of SMAD3 induces human MSC recruitment, which is regulated by primary cilia [61].

Primary cilia perception in bone

Mechanosensing roles of primary cilia

Mechanical stimulation is one of the most important factors in bone modeling and remodeling [3]. Bone cells need mechanical stimulation to maintain their survival and vitality. The lack of mechanical loading results in the apoptosis of bone cells and may lead to the initiation of bone resorption [62]. Bone lacunae and canaliculi are fluid-filled channels that house osteocytes; the latter obtain nourishment and communicate with neighboring osteocytes and osteoblasts from and through fluid [63,64]. Daily walking, running, or jumping creates normal cycles of tension and compression in long bones. Microdeformation generates strain gradients in the medullary cavity, resulting in the development of hydrostatic pressure and fluid flow through lacunae and canaliculi [65]. The fluid in the osteocyte network sloshes back and forth, thus generating membrane-deforming shear forces on the osteocyte network [66,67]. Bone cells detect loading or fluid flow through the cell body and dendritic process and cilial bending [68] and react accordingly to initiate downstream signals. *In vitro* experiments have indicated that oscillating fluid shear (OFS) can promote MSC proliferation, differentiation, and early osteogenesis [69–72]. Mechanical stimulation induces the osteogenesis of periosteal progenitor cells with an increase in osteogenic markers [66]. When human MSCs (hMSCs) are exposed to fluid shear (FS), the expression of bone formation markers increases [73,74]. By contrast, simulated microgravity inhibits the proliferation, osteoblastic, differentiation, and mineralization of rat calvarial osteoblasts (ROBs) [75].

In 2001, Praetorius first proved that primary cilia in the kidney are mechanically sensitive and respond to bending with calcium entry [76]. In 2003, Whitfield proposed that in osteocytes, cilia act as mechanical sensors and bend in response to pulses of extracellular fluid that are generated during walking and running cycles [66]. Malone *et al*. also suggested in 2007 that cilia on bone cells possess physical properties that are consistent with a flow-sensing function [12]. Primary cilia have been proven to perceive hydrostatic pressure applied on the cell body [77] and mediate mechanosensing in bone-like cells [33]. The loading-induced activation of the periosteal bone surface necessitates primary cilia, thereby initiating the recruitment of progenitor cells and osteogenic differentiation [78]. Mechanical stimulation also affects the formation of primary cilia. Simulated microgravity abrogates the formation of primary cilia and decreases the proportion of ciliated ROBs. Residual cilia visibly shorten and appear dotted [75].

With intact primary cilia, periosteal osteochondroprogenitors (OCPs) show an immediate osteogenic response to fluid shear [79]. Primary cilia regulate the oscillatory fluid flow (OFF)-induced expression of osteogenic markers. The levels of markers, such as osteopontin (OPN), cytokine prostaglandin E2 (PGE2), and COX2, significantly increase in MC3T3-E1 osteoblasts and MLO-Y4 osteocytes after exposure to OFF [12]. Osteoblasts, osteoclasts, and OPCs with intact primary cilia increase the levels of PGE2, COX2, OPN, and RUNX2 in response to physical stimulation, but these changes are absent from cilium-blocked cells [14,79]. PGE2 is considered as the first component of the activation cascade in osteocytes during the initiation of bone mechanosensing, and primary cilia induce the release of PGE2 in response to fluid flow [12,62,80]. The damage or removal of cilia by chloral hydrate suppresses the release of PGE2 and the deposition of calcium [81]. In addition, primary cilia regulate the mechanical stimulation-induced expression and secretion of RANKL and OPG from osteocytes, which regulate the differentiation of osteoclasts [82]. A brief summary is shown in Fig. 3.

The length of primary cilia is also sensitive in response to overloading or detecting subtle forces. Delainesmith *et al*. showed that primary cilia on MLO-A5 cells subjected to OFF shorten and become stub-like [81]. Liu *et al.* proved that drag force and torque in a cilium with a length of 8 μm are significantly greater than those in a cilium with a length of 2.5 μm [83]. Overloading decreases the length of primacy cilia or even disassembles cilia on chondrocytes [84]. Nonloaded tendon cells show increased cilia length, which decreases with loading [85].

KIF3a is one of the subunits of the anterograde directed kinesin-II motor protein, and the disruption of KIF3a leads to inappropriately assembled and truncated primary cilia [86]. The disruption of KIF3a in osteoblasts leads to an

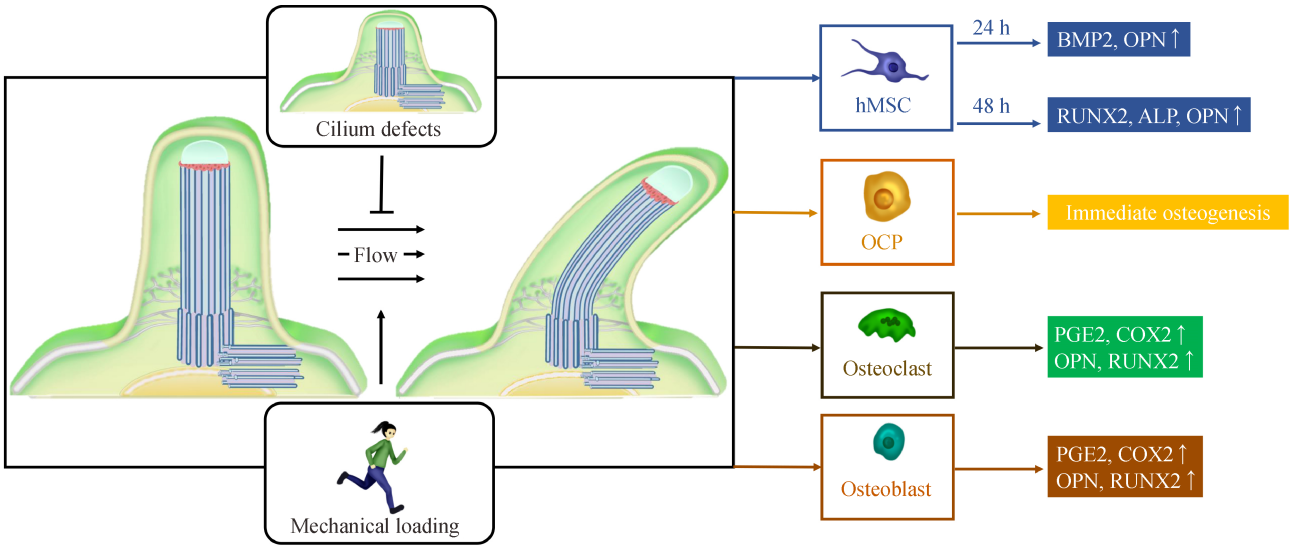

Fig. 3 Mechanical loading sensing by primary cilia in the skeleton. Primary cilia play important roles in mediating mechanical sensing processes in bone cells. The expression of BMP2 and osteopontin OPN, RUNX2, and ALP are upregulated when intact primary cilia are physically stimulated upon the exposure of hMSCs, osteoclasts, and osteoblasts to FS. OCPs show an immediate osteogenic response to FS.

attenuated response to fluid FS stress *in vitro* and impaired cilium-related signaling pathways, such as Hh and Wnt [87]. The loss of KIF3a decreases the number and length of primary cilia [31] and results in the loss of cilia on MSCs. The conditional silencing of *Kif3a* results in severe patterning defects in the craniofacial area, a split sternum, and polydactyly [88]. The specific deletion of cilia or KIF3a in osteoblasts and osteocytes results in a decrease in loading-induced bone formation. After exposure to cyclic ulnar loading, new bone formation in *2.3-Cre;Kif3a*$^{fl/fl}$ mutants is significantly reduced compared with that in the control group [89]. *Col1-Cre;Kif3a*$^{fl/fl}$ mice lacking primary cilia show impaired cellular mechanical sensing and osteogenesis in the area around the implant. Loading-induced bone repair is also impaired in the peri-implant zone with the attenuation of cell proliferation and the deposition and synthesis of collagen fibers along the strain field. This research also suggested that primary cilia influence the strain-induced orientation of cells and the matrix [90].

Ca^{2+} signaling in primary cilium-related sensing

Calcium is one of the most important cations in the human body and plays an important role as a second messenger in signal transduction. Intracellular Ca^{2+} ion concentrations are regulated by a variety of ion pathways, including mechanically sensitive Ca^{2+} channels and transient receptor potential (TRP) channels, that are activated at the cell membrane. TRP channels are categorized into 7 families: TRPC (canonical), TRPV (vanilloid), TRPM (melastatin), TRPA (ankyrin), TRPP (polycystin), TRPML (mucolipin), and TRPN (*Drosophila* NOMPC) [91]. Most TRP channel proteins have selective permeability for calcium ions and respond to the osmotic pressure and pH of the extracellular environment.

TRPV4 regulates the response of renal epithelial cells to osmotic pressure [92]. TRPV4 acts as a mechanical sensor in osteocytes and chondrocytes and mediates cellular response to loading and MSC response to mechanical stimuli [93]. TRPV4 is also expressed on the surfaces of osteoclasts [94]. TRPV4 regulates osteogenesis and osteoclast activity by mediating the localization of NFATc1 to the nucleus [72,95], activating a key signaling pathway in osteogenesis, and promoting osteogenic differentiation [96]. NFATc1 can also act downstream of RANKL, thus promoting the terminal differentiation of osteoclasts [97]. The osteogenic potential of MSCs isolated from *Trpv4*-knockout mice is inhibited [98]. TRPV4 is required in the mechanical transduction of MSCs, Ca^{2+} signaling induced by OFS, and the expression of early osteogenic genes [93]. TRPV4 affects the terminal differentiation of osteoclasts, and *Trpv4*$^{-/-}$ mice exhibit an increase in bone mass compared with the control group [95]. TRPV4 deficiency prevents nonloading-induced decreases in bone mass and bone formation rate and inhibits osteoclast proliferation [94]. Masuyama *et al.* showed that the activation of TRPV4 by drugs enhances osteoclast activity and decreases bone mass [99]. However, they did not subject mice to loading in this experiment. TRPV4 is expressed in highly stressed areas of the cell membrane surface, especially primary cilia [93,100,101]. TRPV4 function requires the existence of an intact cilia structure [101]. Some TRPV4 agonists or drugs, such as

lithium chloride, hydrogen sulfide, and interleukin-1, can be used to extend primary cilia on the surfaces of bone cells [102,103]; enhance the level of mechanical stimulation; and possibly amplify the osteogenic response to prevent bone loss from disuse.

PC1 is a cell-surface-expressed G protein-coupled receptor that is encoded by the *PKD1* gene [104], and PC2 is a TRP-type Ca^{2+}-permeable nonselective cation channel that is encoded by *PKD2*. PC2 interacts with PC1 in a functional complex that is often implicated in a common signaling pathway [105]. PC1 is part of the mechanosensing complex in renal epithelial cells. When the extracellular domain of PC1 is activated in response to fluid flow, the PC2 ion channel opens, allowing Ca^{2+} influx. This intraciliary Ca^{2+} influx is thought to lead to the release in intracellular calcium stores from the ER [106]. Homozygous mutant $Pkd1^{m1Bei/m1Bei}$ mice show delays in intramembranous and endochondral bone formation, and heterozygous Pkd^{m1Bei} mice demonstrate osteopenia with decreases in *Runx2-II* and *osterix* expression, indicating that this phenotype is caused by osteoblast dysfunction [11]. PC1 is also expressed in osteocytes and participates in mechanical transduction, playing important roles in bone development and homeostasis [11]. Mice with PC1 deficiency display reduced loading-induced bone formation in response to mechanical loading [107]. Knocking down *Pkd1* in osteoblasts leads to enhanced adipogenesis, which is similar to the effect of *kif3a* knockdown [87,108]. Interestingly, the further deletion of *kif3a* in *pkd1*-deficient mice reverses skeletal abnormalities by restoring the balance between osteogenesis and adipogenesis [108]. However, the mechanism of this reversal is elusive.

Studies on PC2 in different tissues have provided different results. Jin *et al*. suggested that Ca^{2+} signaling in mouse kidney LLCPK cells induced by mechanical loading requires the presence of primary cilia and PC2 [109], whereas Malone *et al*. demonstrated the opposite results: Ca^{2+} signaling in MC3T3-E1 osteoblasts and MLO-Y4 osteocytes induced by fluid flow is independent of cilia and PC2 [12]. These results are identical to those of Lee *et al.* [100]. Other experiments found that Ca^{2+} influx is absent from MC3T3-E1 cells after stimulation by fluid flow [110]. These results suggest that the role of primary cilia in mechanically induced Ca^{2+} influx is tissue-specific, which may be related to the different types of Ca^{2+} channels in the cell membrane and primary cilia.

Induction of primary cilia by electromagnetic field signals

The fluid in the osteocyte network sloshes back and forth, thus generating streaming ion potentials and piezoelectric currents on the osteocyte network [66]. Electromagnetic fields (EMFs) have been shown to prevent bone loss because of disuse or ovariectomy in mice and can replace medicine for osteoporosis treatment [111–113]. The Food and Drug Administration reported that PEMFs are a safe and effective way to treat osteoporosis [114]. However, the optimal parameters, such as frequency and intensity, and internal mechanism of this treatment need to be further clarified. PEMFs can promote the proliferation, mineralization, and maturation of ROBs [115], and PEMF or electrical field stimulation (EFS) can increase the expression of the osteogenic markers BMP2, COL1, and RUNX2 [35,115]. These processes require the participation of primary cilia. PEMFs promote osteogenesis through the activation of the soluble adenylyl cyclase (sAC)/cAMP/PKA/cAMP response [116], and sAC and p-PKA also localize to primary cilia [117]. After inhibiting primary cilia with iRNA, the promoting effect of 50-Hz PEMFs on osteogenesis differentiation and maturation is abrogated [115]. Yan *et al*. used *IFT88* siRNA to inhibit primary cilium synthesis, leading to significantly decreased expression levels of osteogenic and mineralization marker genes in ROBs [115]. Cai *et al*. showed that primary cilia act as sensors for EFS, which can enhance the osteogenic response in osteoprogenitor cells by simultaneously upregulating the expression of mRNA in ciliary structure proteins and PKD1 [35]. Wnt10b is localized to the base of primary cilia and disappears or is released after sinusoidal EMF (SEMF) treatment. Zhou *et al*. found that 50 Hz 1.8 mT SEMFs increase peak bone mass *in vivo*, enhance the expression of *Wnt10b*, and activate Wnt10b/β-catenin signaling, thus promoting the expression of osteogenic-related proteins. This process is abolished when ciliary synthesis is inhibited [118].

Furthermore, EFS changes the oscillation patterns of cytoplasmic Ca^{2+} [119–121], and the defects of primary cilia do not decrease EFS-induced Ca^{2+} influx [35]. The transduction of EFS signaling through primary cilia in hASCs is independent of stretch-activated channels but may depend on a voltage-gated calcium channel [35]. After blocking voltage-activated calcium channels, the electrical stimulation-induced osteogenic response is completely eliminated [122–124]. These results may provide a theoretical basis for the treatment of bone loss by EFS-assisted drugs that act on ion channels.

Primary cilium-related bone diseases

Ciliopathy is a hereditary disease that affects almost every important organ and tissue [125,126], including the brain, kidney, retina, liver, and bone, manifesting as intracranial cysts and microcephaly [22], autosomal dominant polycystic kidney disease [16], and retinal dystrophy and degeneration [127], suggesting the importance of primary cilia in development and body function. Cilium deficiency in the skeletal system is classified as primary cilium-related bone disease [128]. The main clinical features of these

diseases include shortened long bones, polydactyly or brachydactyly, short or horizontal ribs, reduced rib cage volume, conical epiphyses, and facial deformities.

Bone defects in primary cilium-related syndromes

Generally, cilium-related bone diseases develop as syndromes. Among the best-studied ciliopathies are Mainzer–Saldino syndrome (MZSDS [OMIM 266920]), oral–facial–digital syndrome (OFD), Bardet–Biedl syndrome (BBS [MIM 209900, MIM 613610, MIM 614099]), Sensenbrenner syndrome or cranioectodermal dysplasia (CED [MIM 218330]), and short rib–polydactyly syndromes (SRPs). SRPs are divided into six subgroups: Saldino–Noonan syndrome (SRP type I [OMIM 263530]), Majewski syndrome (SRP type II [OMIM 263520]), Verma–Naumoff syndrome (SRP type III [OMIM 263510]), and Beemer–Langer syndrome (SRP type IV [OMIM 26986]). The other two are Jeune syndrome (also known as Jeune asphyxiating thoracic dysplasia (JATD) [OMIM 611263, OMIM 613091, OMIM 613819, OMIM 614376]) and Ellis–van Creveld (EvC [OMIM 225500]) [16,38,129–131]. Some diseases with known phenotypes and pathogenic genes are shown in Tables 1 and 2.

The typical skeletal phenotypes of SRPs are short ribs, a constricted thoracic cage, metaphyseal dysplasia, and a trident aspect of the acetabular roof. Some cases manifest with defective ossification in the calvaria, vertebrae, and the bones of the hands and feet [38,132]. Polydactyly is consistently observed in SRP type II and EvC, common in types I and III, and rare in type IV and JATD [133]. SRPs differ by variable visceral malformations and metaphyseal appearance [134]. SRP type I is characterized by severely shortened and flipper-like limbs and the transposition of the great vessels and atretic lesions of the gastrointestinal and genitourinary systems [132], and type II presents with a malformed epiglottis and larynx [135]. SRP type III is accompanied by multiple anomalies of major organs, including the heart, intestines, genitalia, kidneys, liver, and pancreas [136,137], and type IV shows brain defects; absent internal genitalia; and renal, bile, and pancreatic cysts [138].

Compared with that of other SRPs with high mortality caused by cardiopulmonary failure, the survival rate of JATD is 40%–80% [139,140]. JATD and SRP types I–IV have typical phenotypes of the skeletal system, such as shortened ribs and bell-shaped thorax, but patients with JATD have a lower probability of having respiratory insufficiency [141]. Other manifestations are short bones, polydactyly, irregular spurs on the acetabular bone and metaphysis, and cone-shaped epiphyses [141–144]. Surviving patients occasionally present retinal degeneration, polycystic kidneys, and hepatopathy [145]. Similar to patients with JATD, individuals affected with MZSDS present cone-shaped epiphyses and retinal dystrophy but also have occasional deformities in other organs, such as cerebellar ataxia, abnormal proximal femur, and liver fibrosis [141,146].

CED is characterized by abnormal ectodermal manifestations, including short fingers, sparse hair, and malformed teeth [147]. In addition, patients with CED have similar clinical phenotypes as patients with Juene syndrome, namely, short stature, short limbs, short ribs, asphyxiate thorax, polydactyly, renal failure, and liver fibrosis. The potential pathogenic genes of CED are still being explored [148]. Walczak-Sztulpa *et al*. stained cultured fibroblasts from patients with CED and found significantly reduced cilium frequency and length in fibroblasts [148]. Gene scanning showed that hypomorphic mutations in *IFT122*, whose production is a component of the primary ciliary IFT-A complex, cause an abnormal ciliary phenotype in homozygous carriers. Furthermore, an abnormal phenotype similar to that in patients with CED is observed in zebrafish embryos with *ift122* knockout [148]. Other cases show the overlap of these cilium-related bone disease phenotypes, indicating interplay among ciliary genes that affect multiple downstream signaling pathways [129,141].

Pathogenic genes in cilium-related bone diseases

Case reports and gene testing data show that common pathogenic genes for cilium-related bone diseases include the IFT protein, dynein, and the basal body protein of primary cilia. Typical mutant genes include components of the transport complex, such as *IFT122*, *IFT43*, *WDR35*, *WDR19/IFT144*, *TTC21B/IFT139*, *IFT140*, and *WDR56/IFT80*; the dynein component genes *DYNC2H1* and *NEK1*; and the basal body protein genes *EVC* and *EVC2* (Fig. 4).

Abnormalities in different ciliary components lead to different phenotypes. The alteration of the IFT-A component disorganizes the assembly and/or maintenance of the ciliary structure by impairing retrograde IFT through the redistribution of ciliary proteins. The staining of the axonemes of fibroblasts from IFT144-deficient individuals revealed a significant reduction in the number of ciliated cells and shortened cilia length [149]. The mutation of IFT140, a core protein of the IFT-A complex, results in shortened primary cilia and the accumulation of IFT-B proteins at the bases of cilia [150]. The mutation of IFT-B genes often leads to loss of cilia [29]. For example, the silencing of *IFT80* causes the shortening or loss of cilia [31]. Chondrocytes from affected individuals with mutant *DYNC2H1*, a cytoplasmic dynein involved in retrograde transport, have shortened primary cilia with bulbous distal ends or no discernible cilia projecting from cell surfaces. In *DYNC2H1* mutants, the early stage of cilial formation remains intact, and the basal body is normally anchored at the plasma membrane, whereas the elongation and/or maintenance of the axoneme by IFT-A required to form the

Table 1 Phenotypes and genes currently known to be involved in primary cilium-related bone diseases with skeletal deformities

Diseases	Mutant genes	Clinical manifestation	
		Craniofacial deformity	Skeletal deformity
MZSDS	IFT140, IFT172	No reports found	Cone-shaped epiphyses of phalanges
OFD			
OFDI	CXORF5	Lobed tongue; tongue nodules; median pseudoclefting of the upper lip; clefts of the palate and tongue; micrognathia; abnormal dentition; telecanthus; hypoplasia of the alae nasi	Syndactyly; branchydactyly
OFDVI	C5ORF42	Cleft or hamartoma of the tongue; micrognathia; additional frenula; cleft lip/palate	Polydactyly; skeletal dysplasia
Sensenbrenner syndrome/CED	WDR19, IFT122, WDR35, SPAGE17, IFT43	Dolichocephaly; high forehead; full cheeks; telecanthus; hypodontia and/or microdontia	Narrow thorax; brachydactyly; short limbs
Weyers acrofacial dysostosis	IFT80, EVC, EVC2	Median cleft; conical teeth; fused teeth; abnormal shape and number of lower and upper incisors; hypodontia; enamel hypoplasia	Postaxial polydactyly; mild shortness of stature with short limbs
SRPs[a]			
SRPI	Unknown	Cleft lip/palate; lobed tongue	Postaxial polydactyly (++); severely shortened and flipper-like limbs; striking metaphyseal dysplasia of tubular bones; defective ossification in the calvaria, vertebrae, pelvis, and bones of the hands and feet
SRPII	DYNC2H1, NEK1	Cleft lip/palate	Pre- and postaxial polysyndactyly (+++); short and narrow thorax with horizontally oriented ribs; short tubular bones with smooth ends; tibial agenesis or ovoid tibiae shorter than fibulae
SRP III	IFT80, DYNC2H1	Cleft lip/palate	Polydactyly (++); extreme narrowness of the thorax; severely shortened tubular bones with round metaphyseal ends and lateral spikes
SRP IV	Unknown	Flat face; hamartoma of the tongue; lobed tongue; cleft lip/palate; natal tooth	Polydactyly (+); short and narrow thorax with horizontally oriented ribs; small iliac bones; short tubular bones with smooth metaphyseal margins; bowed radii and ulna
EVC	EVC, EVC2	Dysplastic teeth; natal tooth; labiogingival adhesions	Polydactyly (+++); short ribs; short limbs
ATD	WDR34, IFT80, DYNC2H1, TTC21B, WDR19	Dental abnormalities	Inconstant polydactyly; short ribs and limbs; short stature; trident acetabular roof
SRP type V	WDR35	Facial abnormalities	Polydactyly (+); acromesomelic hypomineralization; and campomelia
BBS	BBSome1–19	Brachycephaly/macrocephaly; bitemporal narrowing; male frontal balding; short and narrow palpebral fissures; long shallow philtrum; nasal anomalies; dental crowding; midfacial hypoplasia; mild retrognathia	Postaxial polydactyly
JS	INPP5E, ARL13B, CC2D2A, RPGRIP1L, TMEM67, NPHP1, AHI1, CEP290, CXORF5, TMEM216…	Large head and frontal prominence; arched eyebrows; drooping upper eyelids; widened eyes; low ears; triangular mouths; cleft lip/palate	Polydactyly (10%–15%); scoliosis

MZSDS, Mainzer–Saldino syndrome; OFD, oral–facial–digital syndrome; CED, cranioectodermal dysplasia; SRP, short rib–polydactyly; EVC, Ellis–van Creveld syndrome; ATD, asphyxiating thoracic dystrophy; BBS, Bardet–Biedl syndrome; JS, Joubert syndrome.

Table 2 Abnormal phenotypes of primary cilium-related bone diseases in organs other than the skeletal system

Diseases	Mutant genes	Other deformities
MZSDS	IFT140, IFT172	Chronic renal failure; retinal dystrophy; cerebellar ataxia
OFD		
OFDI	CXORF5	Cystic renal disease
OFDVI	C5ORF42	Mental retardation; cerebellar anomalies; conductive loss of hearing; congenital heart anomalies; micropenis; cryptorchidism
Sensenbrenner syndrome/CED	WDR19, IFT122, WDR35, SPAGE17, IFT43	Ectodermal manifestations, including sparse hair, abnormal nails, skin laxity, and bilateral inguinal hernia; nephronophtisis, hepatic fibrosis, retinitis pigmentosa, and/or brain anomalies
Weyers acrofacial dysostosis	IFT80, EVC, EVC2	Hypoplastic and dysplastic nails
SRPs		
SRPI	Unknown	Polycystic kidney; transposition of great vessels; atretic lesions of the gastrointestinal and genitourinary systems
SRPII	DYNC2H1, NEK1	Malformed epiglottis and larynx; renal cysts; genital, cardiac and intestinal abnormalities
SRP III	IFT80, DYNC2H1	Anomalies of the heart, intestine, genitalia, kidney, liver, and pancreas
SRP IV	Unknown	Brain defects; absent internal genitalia; renal, bile, and pancreatic cysts
EVC	EVC, EVC2	Dysplastic nails; congenital cardiac defects; urogenital anomalies
ATD	WDR34, IFT80, DYNC2H1, TTC21B, WDR19	Retinal degeneration; cystic renal disease; and liver diseases
SRP type V	WDR35	Extreme micromelia; polycystic kidney
BBS	BBSome1–19	Progressive vision loss; polycystic kidney; obesity; retinitis pigmentosa; congenital cardiac defects; learning difficulties
JS	INPP5E, ARL13B, CC2D2A, RPGRIP1L, TMEM67, NPHP1, AHI1, CEP290, CXORF5, TMEM216…	Cerebellar and brainstem malformation with molar tooth sign; ataxia; mental retardation; breathing dysregulation; retinal dystrophy; kidney and liver anomalies

MZSDS, Mainzer–Saldino syndrome; OFD, oral–facial–digital syndrome; CED, cranioectodermal dysplasia; SRP, short rib–polydactyly; EVC, Ellis–van Creveld syndrome; ATD, asphyxiating thoracic dystrophy; BBS, Bardet–Biedl syndrome; JS, Joubert syndrome.

mature primary cilia is abnormal [151]. *DYNC2H1* encodes a subunit of the cytoplasmic dynein complex that is associated with the light intermediate chain (DYNC2LI1) and directly participates in the contact and translocation of the dynein complex along microtubules through its large motor domain [152]. In mammalian tissue, the colocalization of DYNC2H1, DYNC2LI1, and IFT pathway homologs supports the generation and maintenance of cilia [131].

Mutations in genes that encode components of IFT, especially the IFT-A complex, are major causes of skeletal ciliopathies [129,144]. IFT140 is one of the most studied IFT-A genes among disease-related genes. Schmidts *et al*. found that all biallelic *IFT140* patients present with renal disease in early childhood with notable retinal involvement but have a nonlethal thorax-related clinical course and no polydactyly. The *IFT140* mutation has also been detected in patients with JATD [129,153]. At least 6 other genes are related to JATD, namely, *DYNC2H1*, *IFT80*, *IFT139*, *IFT140*, *WDR19*, and *WDR34* [129–131,139–141,144, 149,154,155], indicating a complex correspondence between genotype and phenotype. Schmidts *et al*. concluded that the *IFT140* mutation is a rare cause of JATD in general but is a frequent cause of JATD with renal involvement [141]. In 2012, Perrault *et al.* found that the *IFT140* mutation is the only cause of MZSDS [129]. In the following year, Halbritter *et al.* added *IFT172* (an IFT-B component) to the pathogenic gene list [156]. *IFT140* and *IFT172* are the only two pathogenic genes found in MZSDS to date. Studies on mouse models of gene mutations and knockouts have found that *Ift140* mutant or *Ift140*-knockout mouse embryo development is slower than wild-type embryo development with the highest fatalities in midpregnancy and that survivors present with

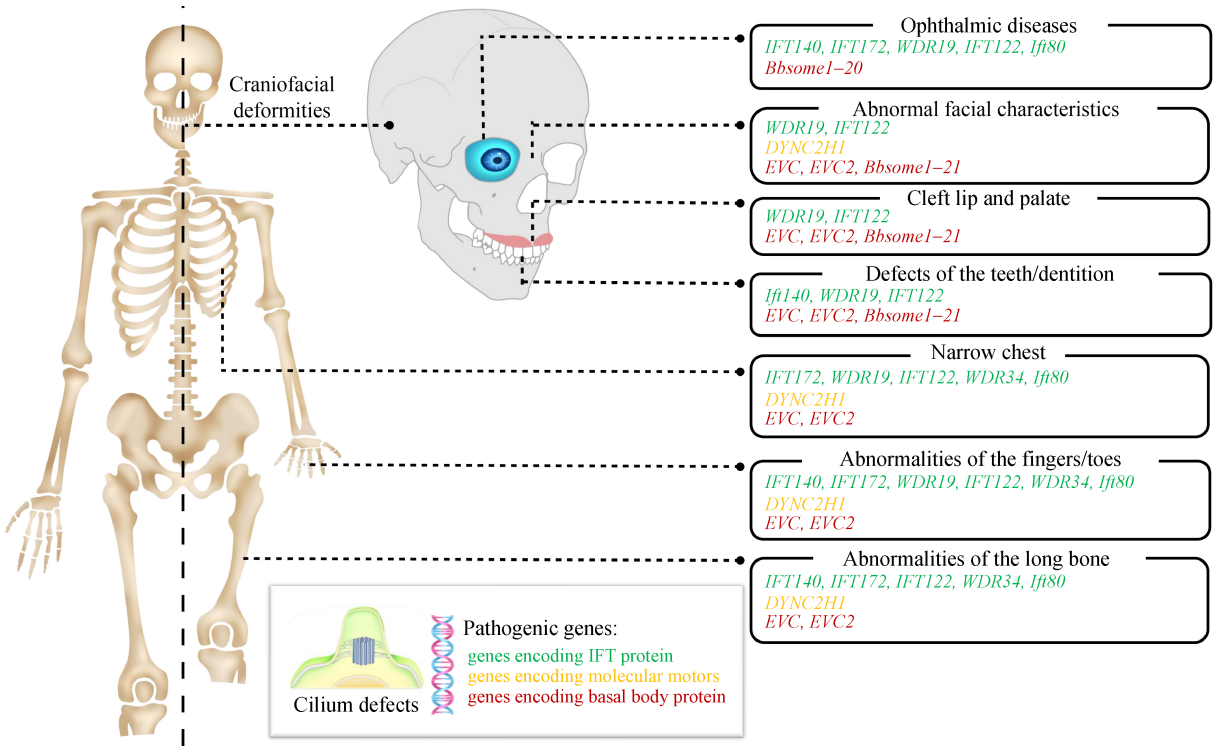

Fig. 4 Bone and craniomaxillofacial abnormalities in ciliopathies. Ciliopathies affect the brain, kidneys, retina, liver, and bone. The main clinical features of skeletal ciliopathies include the shortening of the long bones, the abnormalities of the fingers/toes, a narrow chest, and craniofacial deformities (including ophthalmic diseases, abnormal facial characteristics, cleft lip and palate, and defects of the teeth/dentition). Genes encoding IFT (green), molecular motors (yellow), and the basal body proteins (red) of primary cilia are common pathogenic genes in skeletal ciliopathies. Studies on Ift140, Ift80, and Evc in mice have revealed similar skeletal phenotypes, and ift172 and ift122 in zebrafish show similar phenotypes in terms of facial manifestation.

exencephaly with polydactyly. Other skeletal deformations include severe rib defects, failed calvarial development, and cervical vertebral fusion [153]. The conditional knockdown of *Ift140* in different cells leads to different phenotypes. For example, the deletion of *Ift140* in renal collecting ducts results in severe early cystic kidney disease [143]. After the knockout of *Ift140* in osteoblast precursor cells, mice are smaller in size and weight than wild-type mice and have reduced expression levels of genes involved in bone formation and osteogenic processes [157].

IFT80 and DYNC2H1 have been verified to be associated with JATD and SRP type III [131,151,154]. Rix *et al*. established a model of $Ift80^{gt/gt}$ mice and found that the percentage of survival to birth is less than 3%. Postnatal survivors present marked growth retardation, constricted thoracic cages, ribs with irregular margins between bone and cartilage, shortened long bones, and a characteristic bilateral preaxial polydactyly of the hind limbs wherein a single extra digit is formed and is markedly longer than the other digits [130]. Defects in cytoskeletal microtubule architecture are also observed in mutant SRP chondrocytes with an approximately 2-fold increase in acetylated α-tubulin in the SRP samples relative to that in the control. The abnormalities identified in SRP raise the possibility that the loss of DYNC2H1 function may affect the movement of organelles and the transport of critical cargo necessary for signal transduction and skeletal development [151]. Merrill *et al.* speculated that homozygosity with two null alleles results in early embryonic lethality, whereas a combination of a null mutation and a variety of missense mutations may lead to a range of phenotypes [151].

WDR34 concentrates mostly around the centrioles and basal body and is considered as a linker between cytoplasmic dynein-1 and IFT dynein-2 motors [144]. Cases with mutations in WDR34 may account for up to 10% of all JATD cases [144]. A previous report demonstrated that WDR34 inhibits the NF-κB pathway component TAK1 in cell culture [158]. The mutation of the *WDR34* homolog *dync2i1* in zebrafish leads to a typical ciliopathic phenotype [159]. However, whether the axonemal localization of WDR34 may be affected in these deficient cells remains unclear [144]. The proportion of ciliated cells and cilial length are not significantly affected in any of the *Wdr34*-knockdown ATDC5 cell lines

(mouse chondrocyte progenitor cells) [144]. This finding is similar to the results reporting the absence of loss or malformation of cilia in the Ift80-deficient hypomorphic JATD mouse model, in which a low level of Ift80 expression allows ciliogenesis but does not rescue Hh signaling defects [130]. The achieved level of WDR34 knockdown may not be sufficient to result in a ciliogenetic defect [144]. Altogether, the function of WDR34 in the IFT dynein-2 complex remains to be further investigated.

EVC, the basal body protein, is unnecessary for ciliary synthesis. $Evc^{-/-}$ mice show growth plate dysplasia of the long bones but retain normal Ihh expression in the growth plate; however, the expression of the downstream genes Ptch1 and Gli1 is significantly reduced [160]. Evc/Evc2 defects lead to the failure of Sufu/Gli3FL dissociation, and Gli3R increases after treatment with the Smo agonist SAG [161]. The functions of primary ciliary genes are summarized in Table 3.

Table 3 Function of primary cilium-related genes and mutant model with deformities

Genes	Encode protein	Function	Mutant model	Deformity
Basal body				
BBSome1–21	BBS1–21	BBS1, BBS2, BBS4, BBS5, BBS7, BBS8, and BBS9 along with an interacting protein BBIP 10 form a complex called the BBSome, which is involved in ciliary membrane biogenesis	Knockdown of *bbs1* in zebrafish	Disruption of Kupffer's vesicle formation, heart laterality defects (jogging and looping), and delay in melanosome retrograde transport
			Mouse BBS model (*Bbs7* and *Ift88*^{orpk} double mutants)	Embryonic lethality
		BBS4, BBS6, and BBS8 are expressed in ciliated epithelia and localize to the centrosome and basal bodies	Mouse BBS models (*Bbs4*$^{-/-}$and *Bbs6*$^{-/-}$)	Increased face width, upward nasal displacement, midfacial flattening, and retrognathia
			bbs4, *bbs6,* and *bbs8* zebrafish morphants	Shortened anterior neurocranium, reduced mandibles, and few hypoplastic branchial arches
EVC	Evc and Evc2	Evc and Evc2 are mutually required for localizing to primary cilia and for maintaining their normal protein levels	Mouse BBS model (*Evc*$^{-/-}$)	Decreased Ptch1 and Gli1 expression, delayed bone collar formation, and advanced chondrocyte maturation in the growth plate
EVC2	Evc and Evc2	Evc and Evc2 are mutually required for localizing to primary cilia and for maintaining their normal protein levels	Mouse BBS model (*Evc2*$^{-/-}$)	Reduced Ptch1, Gli1, and Pthrp expression; distalward shortening of the limbs and short ribs; delayed perichondrial osteoblast differentiation in the mutant growth plate
CXORF5	OFD1	Maintaining the microtubule length stability of centrioles	*OFD1*-mutated human (formerly named "*Cxorf5/71-7a*")	Craniofacial anomalies (facial skin milia and broadened nasal ridge), facial asymmetry and oral anomalies (hamartomas, clefts of the lip and palate, and dental abnormalities)
Transition zone				
CEP290 (also known as *NPHP6* and *MKS4*)	CEP290	CEP290 controls ciliary protein composition and signaling	*CEP290* nonsense mutations in fibroblast cells	Cilial elongation, impaired ciliogenesis, and ciliary composition defects
Motors				
DYNC2H1	DYNC2H1	DYNC2H1 plays a role in retrograde transport in the cilia. The loss of DYNC2H1 function can affect the movement of organelles and the transport of critical cargo necessary for signal transduction and skeletal development	*DYNC2H1*-mutated human	Perinatal lethality, skeletal disorders, polydactyly and multisystem organ abnormalities; shortened cilia and abnormal cytoskeletal microtubule architecture in chondrocytes
WDR34	WDR34	WDR34 is a dynein intermediate chain that is associated with the retrograde IFT motor	*WDR34*-mutated human	Protruding abdomen, narrow thorax, short horizontal ribs, acetabular spurs, shortened femora, and handlebar clavicles

(*Continued*)

Genes	Encode protein	Function	Mutant model	Deformity
IFT				
IFT122	IFT122	Part of IFT-A	Loss of ift122 in zebrafish	Shortened body axis and curvature, cardiac edema, and small eyes
IFT140	IFT140	Part of IFT-A	Mouse model (*Ift140* mutant or knockout)	Perinatal lethality, slowed embryo development, exencephaly, polydactyly, severe rib defects, calvarial development failure, and cervical vertebral fusion
TTC21B/IFT139	IFT139	Part of IFT-A	*ttc21b* tb-MO in zebrafish	Shortening of the embryonic axis, widening and kinking of the notochord, broadening and thinning of the somites
WDR19	IFT144	Part of IFT-A	*WDR19*-mutated human	Skeletal anomalies, chronic renal failure, and retinitis pigmentosa
IFT172	IFT172	Part of IFT-B	Knockdown of *ift172* in zebrafish	Ventral body axis curvature, kidney cysts, otolith defects, retinal degeneration, hydrocephaly, and ciliogenesis defects
IFT80	IFT80	Part of IFT-B	Mouse model ($Ift80^{gt/gt}$)	Embryonic lethality, growth retardation, constricted thoracic cages, shortened long bones, and characteristic bilateral preaxial polydactyly

Roles of primary cilia in craniofacial development

Craniofacial bones, as components of the skeletal system, have similar structural characteristics as bones in other parts of the body but undergo unique and complex developmental processes. As the embryo differentiates, neural crest (NC) cells in the ectodermal germ layer undergo epithelial-to-mesenchymal transition and migration. NC cells then differentiate into facial bones, cartilage, and teeth (except enamel). The entire process involves many different signaling pathways, such as BMP, FGF, and Wnt, which together establish a regulatory network and play essential roles in the evolution of NC [162]. The connection between primary cilia and many developmental signaling pathways is critical for craniofacial development [163]. More than 30% of ciliopathies are characterized by craniofacial phenotypes, including midfacial hypoplasia, cleft lip and palate, retrognathia, and craniosynostosis. The frequency and severity of craniofacial phenotypes underscore the importance of cilia during the development of craniofacial complexes [128]. Several important cilium-related craniofacial syndromes exist.

Primary cilium-related craniofacial syndromes

JS and JS-related disease (JSRD) are a group of stunted growth/multiple congenital abnormality syndromes that are characterized by molar tooth sign in the brain. JS is a complex midbrain–hindbrain deformity. JS manifests with unique features in the facial area, including a large head and frontal prominence, arched eyebrows, drooping upper eyelids, wide eyes, low ears, and a triangular mouth. Currently, mutations in approximately 34 genes have been identified to be related to JS [164]. These mutations include *INPP5E*, *ARL13B*, *CC2D2A*, *RPGRIP1L*, *TMEM67*, *NPHP1*, *AHI1*, *CEP290*, *CXORF5*, and *TMEM216* [128], with *CEP290* (also known as *JBTS5*) being the most common. The protein encoded by *CEP290* is located in the cilial transition zone. *CEP290* mutant cells have the typical characteristics of elongated cilia, impaired ciliogenesis, and cilia composition defects. Some studies have proposed that targeted exon skipping provides new directions for JS treatment because it is capable of rescuing the expression of CEP290 protein, the composition defects of ciliary proteins, and the function of the transition zone in *CEP290* mutant cells [165].

The OFD syndrome lineage includes 13 different genetic diseases. OFD type I ([OMIM311200]) is an X-linked dominant disorder with an incidence of approximately 1/50 000, with affected males dying during pregnancy. Its symptoms are mainly manifested in the oral cavity (lobulated tongue, tongue nodules, clefts of the hard or soft palate, accessory gingival frenulae, hypodontia, and other dental abnormalities) and the face (widely spaced eyes or telecanthus, hypoplasia of the alae nasi, median cleft or pseudocleft upper lip, and retrognathia) [166]. Genetic linkage analysis and familial analysis of OFD type I cases have revealed that this syndrome is caused by a mutation in the *CXORF5* gene located in the Xp22.2

chromosome. The product of this gene is OFD1, one of the fundamental proteins of the primary cilia, and is located in the basal bodies at the base of the ciliary axoneme. OFD1 is necessary for maintaining the microtubule length stability of centrioles and the recruitment of IFT88 but can be prematurely truncated by mutations in the *CXORF5* gene [167,168]. The clinical characteristics of the pathogenesis of OFD type I are related to abnormal Hh signal transduction, a depressed planar cell polarity pathway, and errors in cell cycle control that result from the dysfunctions of primary cilia [169]. The knockout of *Ofd1* in mice to establish an animal model recapitulates the main symptoms of OFD1, but severity is enhanced [170].

OFD type VI is a rare phenotype of JS and is associated with a *C5ORF42* mutation [171]. The craniofacial features include tongue fissure, tongue hamartoma, retrognathia, additional frenulae, and other mouth–face deformities (such as cleft lip and palate) [172]. In chicken embryos, *C5orf42* silencing results in the widening of the facial midline, the appearance of abnormal primary cilia on the cell surface, and the weakening of cell response to Shh agonists [173].

BBS is an autosomal recessive genetic heterozygous disorder that affects multiple parts of the body. In addition to the common symptoms of progressive vision loss, polycystic kidneys, and postaxial hand polydactyly, patients with BBS may also present with special craniofacial appearances: brachycephaly, macrocephaly, bitemporal narrowing, male frontal balding, large ears, short and narrow palpebral fissures, a long shallow philtrum, nasal anomalies, dental crowding, midfacial hypoplasia, and mild retrognathia [174]. The mutation of *BBS* genes leads to abnormal tooth development, such as crowded dentition, protrusions, and enamel hypoplasia. The clinical examination of patients with BBS revealed tooth dysplasia, microdontia, short roots, or taurodontism [175–177]. To date, 21 pathogenic genes have been discovered (*BBSome1–21*), but the BBS protein network remains to be determined [178]. The 8 subunits of the BBSome assemble into a functional complex and play vital roles in ciliary transport. In contrast to IFT-A or IFT-B mutants, BBS mutants usually do not show significant abnormalities in cilial structure but exhibit abnormal signal transduction in cilia [179]. Zebrafish model studies have shown that the knockout of different BBS genes leads to significant overlapping phenotypes, and the consumption of the BBSome increases the Hh signal in the zebrafish fin bud, leading to skeletal abnormalities [180]. The deletion of the BBSome gene in mice results in the accumulation of Smo and Ptch1 in cilia and the reduction in the Shh response [181].

EvC and Weyers acrofacial dysostosis (MIM 193530) have been proven to be associated with EVC and EVC2 [182,183]. EvC is a rare autosomal recessive disorder that affects bone development due to chondroectodermal dysplasia [128]. Clinical features include short statures, short ribs, polydactyly, nail and tooth dysplasia, and labiogingival adhesions. Affected children have congenital cardiac defects, most frequently a defect in primary atrial septation, which is the common cause of death [184]. EvC shows a wide spectrum of abnormal oral manifestations, including serrated incisal margins, dental transposition, diastema, conical teeth, enamel hypoplasia, and hypodontia. Teeth may be erupted at birth or exfoliate prematurely [185]. Incisor hypoplasia [186], fused first and second molars, molar microdontia, and abnormal root development can be seen in mice lacking *Evc* [187]. Weyers acrofacial dysostosis is an autosomal dominant disorder that is clinically characterized by mild short stature, postaxial polydactyly, and nail dystrophy. Craniofacial phenotypes include ocular hypotelorism; median cleft; enamel hypoplasia; conical teeth; single central incisor or hypoplasia; and, less frequently, other organ abnormalities [188,189]. The differences between EvC and Weyers are the different genetic patterns and the severity of the phenotype [190].

Primary cilia in tooth development

Teeth and bone undergo similar cell maturation processes and mineralized matrix formation [191]. Several studies have observed that primary cilia participate in every stage of tooth development [186,192,193]. At the embryo stage, the thickened epithelium differentiates into dental lamina and extends toward deep connective tissue. Terminal cells proliferate and form the tooth germ. During this period, primary cilia can be observed in epithelial thickening and the mesenchyme below the thickening [186]. The tooth germ is composed of three parts: the enamel organ, which forms the enamel; the dental papilla, which forms the dentin and dental pulp; and the dental sac, which develops into periodontal tissue. Primary cilia are expressed during the three differentiation stages of the enamel organ, dental papilla, and dental sac [186,192]. During the bud and cap stage, cilia are mostly distributed in the epithelial dental tissues and mesenchymal cells surrounding the tooth germ. Interestingly, cilia gather on the apical surface of the basal epithelial layer, whereas few cilia localize in the central area and are short in the bud stage [186]. In the bell stage, the expression of primary cilia is higher in the developing cervical loop [193] and the enamel knot area than in the stellate reticulum [186]. During this stage, the concave surface of the enamel organ displays the shape of the teeth that will form in the future. The enamel knot, the local epithelial thickening in the inner enamel epithelium, may be the signal center and may have important effects on the tooth, especially cusp morphogenesis [194,195]. Primary cilia in enamel knots are longer than in other organs [186]. Considering that cilia are involved in many signaling pathways that regulate growth and development, cilia may

regulate tooth morphology through the expression of signaling pathways in enamel knots.

After the differentiation and maturation of ameloblasts during the late bell stage, undifferentiated mesenchymal cells near the inner enamel epithelium of the dental papilla are induced to grow and differentiate into odontoblasts. The primary cilia on the odontoblasts are aligned parallel to the dentin wall with the axoneme oriented toward the pulp core, and the cilia on the ameloblasts project toward the outer enamel epithelium such that the cilia on the surface of two cells are oriented in the opposite direction distal from the area where hard tissue is produced [192,196]. However, the cilia in the dental follicle or the periodontal ligament (PDL) show no obvious pattern after birth [192], suggesting that primary cilia have an important influence on regulating cell polarity and mineral deposition direction. In early postnatal and adult mice, primary cilia are detected on the edges of the PDL adjacent to the teeth and alveolar bone, and few ciliated cells are observed in the medial region of the PDL [192]. In odontoblasts and ameloblasts, cilia gradually elongate during differentiation, whereas cilia length and frequency decrease on dental stalk cells and rudimental successional dental lamina with keratinization and aging, respectively [186]. A previous *in vitro* study on dental pulp stem cells suggested that primary cilia elongate during odontogenesis and that the ciliated cell population also increases significantly [197].

Single variations in the key components of primary cilia also cause different types of dental dysplasia. Variations in IFT88, the primary cilial component involved in Shh signaling, lead to significant abnormal dental phenotypes. Shh, as the major ciliary signaling pathway, is involved in tooth germ development, growth, formation, and differentiation. Abnormal primary cilia have a pleiotropic effect on tooth development [198]. $Tg737^{orpk}$ is a hypomorphic allele of *IFT88/Polaris* in which mutants have enhanced HH signals and form ectopic molars. The knockout of *Ift88* in mesenchymal cells results in hyperdontia, whereas the knockout of *Ift88* in epithelial cells does not result in the manifestation of the phenotype [199]. The focal domains of WNT and Shh define the sites where teeth will develop; therefore, any changes in expression can cause defects in incisor initiation. In $Wnt1^{Cre+}Kif3a^{fl/fl}$ mice, molar germs are enlarged, and enamel organs are misshapen [186]. Furthermore, HH signaling is lost in the tooth germ, whereas WNT/β-catenin signaling is enhanced in the mesenchyme of $Wnt1\text{-}cre;Kif3a^{f/f}$ mice, resulting in multiple invaginations of the epithelium instead of a single secondary enamel knot [200].

$Ift140^{cauli/cauli}$ embryos exhibit severe craniofacial defects, including absent or rudimentary alisphenoid and palatine and hypoplastic and malpositioned maxilla and premaxilla [153]. Our laboratory found that the cKO of *IFT140* in odontoblasts results in a reduced number of primary cilia. Dentin thickness is thinner and dentin formation is slower in $Osx\text{-}Cre;Ift140^{f/f}$ mice than in the control. *Ift140*-cKO mice have short molar roots and hypoplastic interradicular dentin with the decreased expression of the Shh signaling molecules Ptch1, Smo, and Gli1-3. $Osx\text{-}Cre;Ift140^{f/f}$ mice have impaired reparative dentin formation, whereas the number of primary cilia in the wild-type mice increases after cavity preparation, suggesting that primary cilia act in reparative dentin formation and pulp protection [201].

Tooth regeneration has always been an important topic in the field of dental tissue research. Research on the regulatory factors of dental development during different stages is helpful for researchers to explore key cellular structures and signaling pathways and to find possible methods for tooth regeneration *in vitro*.

Future perspectives

In the last two decades, a complete reversal of the opinion that primary cilia are of no great importance has been gradually accepted. Current studies have concluded that many primary ciliary genes can regulate complex signaling during bone development. Primary cilia also act as mechanical and EMF sensors that detect loading or current and voltage changes in the skeletal system and regulate bone remodeling. However, the biological response and activity mechanism of cilia and cells after external stimuli remain unclear. In the craniofacial area, primary cilia also function in the development of mandibular and intervertebral discs (IVDs). The deletion of IFT80 disrupts Hh signaling and decreases IVD marker gene expression, causing the early onset of the IVD disorder phenotype [202]. The slightly shorter and thicker mandibles of Ift88 mice than those of wild-type mice may be related to altered Hh signaling [203]. With the deepening of the understanding of auxology and the increase in research on genetic diseases, additional secrets regarding ciliary function and mechanisms in craniofacial development will be revealed. These tiny organelles are anticipated to play important roles in metabolic diseases and aging diseases of hard tissue. Research on the regulatory functions of ciliary genes may provide novel information for use in proposing potential therapeutic targets. In conclusion, further comprehensive studies are needed to reveal the biological function of primary cilia.

In addition, the etiology of ciliary hereditary osteopathies is complex, and their pathogenic genes are diverse. Embryonic lethality caused by severe skeletal diseases has introduced difficulties into population screening and animal research. Current screening studies have revealed that most cilium-related bone diseases may have multiple pathogenic genes. An intricate relationship may exist between genes and different genotypes, and multiple areas of genotypes and disease phenotypes overlap. The

underlying mechanism cannot be explained by a single pathway, thus complicating the identification of therapeutic targets and the appropriate timing of treatment and interventions. The pathogenesis and treatment of primary cilium-related bone diseases require extensive long-term genetic screening and animal experiments for further clarification.

Acknowledgements

This work was supported by grants from the National Natural Science Foundation of China (Nos. 82061130222, 81822012, 81771043, 92049201, 81770873, and 81802193), the National Science and Technology Major Project of China (No. 2016YFC-1102705), the Shanghai Academic Leader of Science and Technology Innovation Action Plan (No. 20XD1424000), and the Shanghai Experimental Animal Research Project of Science and Technology Innovation Action Plan (No. 8191101676). We also apologize to the many researchers whose work could not be cited due to the limited scope of discussion in this evolving field.

Compliance with ethics guidelines

Sijin Li, Han Zhang, and Yao Sun declare that they have no conflict of interest. This manuscript is a review article and does not involve a research protocol requiring approval by a relevant institutional review board or ethics committee.

References

1. Berendsen AD, Olsen BR. Bone development. Bone 2015; 80: 14–18
2. Buck DW 2nd, Dumanian GA. Bone biology and physiology: part I. The fundamentals. Plast Reconstr Surg 2012; 129(6): 1314–1320
3. Hadjidakis DJ, Androulakis II. Bone remodeling. Ann N Y Acad Sci 2006; 1092(1): 385–396
4. Clarke B. Normal bone anatomy and physiology. Clin J Am Soc Nephrol 2008; 3(Suppl 3): S131–S139
5. Owen M. The origin of bone cells in the postnatal organism. Arthritis Rheum 1980; 23(10): 1073–1080
6. Walmsley GG, Ransom RC, Zielins ER, Leavitt T, Flacco JS, Hu MS, Lee AS, Longaker MT, Wan DC. Stem cells in bone regeneration. Stem Cell Rev Rep 2016; 12(5): 524–529
7. Scherft JP, Daems WT. Single cilia in chondrocytes. J Ultrastruct Res 1967; 19(5): 546–555
8. Rich DR, Clark AL. Chondrocyte primary cilia shorten in response to osmotic challenge and are sites for endocytosis. Osteoarthritis Cartilage 2012; 20(8): 923–930
9. Wang S, Wei Q, Dong G, Dong Z. ERK-mediated suppression of cilia in cisplatin-induced tubular cell apoptosis and acute kidney injury. Biochim Biophys Acta 2013; 1832(10): 1582–1590
10. Tummala P, Arnsdorf EJ, Jacobs CR. The role of primary cilia in mesenchymal stem cell differentiation: a pivotal switch in guiding lineage commitment. Cell Mol Bioeng 2010; 3(3): 207–212
11. Xiao Z, Zhang S, Mahlios J, Zhou G, Magenheimer BS, Guo D, Dallas SL, Maser R, Calvet JP, Bonewald L, Quarles LD. Cilia-like structures and polycystin-1 in osteoblasts/osteocytes and associated abnormalities in skeletogenesis and Runx2 expression. J Biol Chem 2006; 281(41): 30884–30895
12. Malone AM, Anderson CT, Tummala P, Kwon RY, Johnston TR, Stearns T, Jacobs CR. Primary cilia mediate mechanosensing in bone cells by a calcium-independent mechanism. Proc Natl Acad Sci U S A 2007; 104(33): 13325–13330
13. Federman M, Nichols G Jr. Bone cell cilia: vestigial or functional organelles? Calcif Tissue Res 1974; 17(1): 81–85
14. Yuan X, Serra RA, Yang S. Function and regulation of primary cilia and intraflagellar transport proteins in the skeleton. Ann N Y Acad Sci 2015; 1335(1): 78–99
15. Eggenschwiler JT, Anderson KV. Cilia and developmental signaling. Annu Rev Cell Dev Biol 2007; 23(1): 345–373
16. Fry AM, Leaper MJ, Bayliss R. The primary cilium: guardian of organ development and homeostasis. Organogenesis 2014; 10(1): 62–68
17. Sorokin SP. Reconstructions of centriole formation and ciliogenesis in mammalian lungs. J Cell Sci 1968; 3(2): 207–230
18. Berbari NF, O'Connor AK, Haycraft CJ, Yoder BK. The primary cilium as a complex signaling center. Curr Biol 2009; 19(13): R526–R535
19. Izawa I, Goto H, Kasahara K, Inagaki M. Current topics of functional links between primary cilia and cell cycle. Cilia 2015; 4(1): 12
20. Wheway G, Nazlamova L, Hancock JT. Signaling through the primary cilium. Front Cell Dev Biol 2018; 6: 8
21. Satir P, Christensen ST. Overview of structure and function of mammalian cilia. Annu Rev Physiol 2007; 69(1): 377–400
22. Youn YH, Han YG. Primary cilia in brain development and diseases. Am J Pathol 2018; 188(1): 11–22
23. Desai A, Mitchison TJ. Microtubule polymerization dynamics. Annu Rev Cell Dev Biol 1997; 13(1): 83–117
24. Yoon SY, Choi JE, Choi JM, Kim DH. Dynein cleavage and microtubule accumulation in okadaic acid-treated neurons. Neurosci Lett 2008; 437(2): 111–115
25. Kim S, Zaghloul NA, Bubenshchikova E, Oh EC, Rankin S, Katsanis N, Obara T, Tsiokas L. Nde1-mediated inhibition of ciliogenesis affects cell cycle re-entry. Nat Cell Biol 2011; 13(4): 351–360
26. Cao M, Zhong Q. Cilia in autophagy and cancer. Cilia 2016; 5(1): 4
27. Hu Q, Nelson WJ. Ciliary diffusion barrier: the gatekeeper for the primary cilium compartment. Cytoskeleton (Hoboken) 2011; 68(6): 313–324
28. Christopher KJ, Wang B, Kong Y, Weatherbee SD. Forward genetics uncovers transmembrane protein 107 as a novel factor required for ciliogenesis and Sonic hedgehog signaling. Dev Biol 2012; 368(2): 382–392
29. Satir P, Pedersen LB, Christensen ST. The primary cilium at a glance. J Cell Sci 2010; 123(4): 499–503
30. Rosenbaum JL, Witman GB. Intraflagellar transport. Nat Rev Mol Cell Biol 2002; 3(11): 813–825
31. Yang S, Wang C. The intraflagellar transport protein IFT80 is required for cilia formation and osteogenesis. Bone 2012; 51(3): 407–417
32. Veland IR, Awan A, Pedersen LB, Yoder BK, Christensen ST. Primary cilia and signaling pathways in mammalian development,

health and disease. Nephron Physiol 2009; 111(3): 39–53
33. Yuan X, Yang S. Primary cilia and intraflagellar transport proteins in bone and cartilage. J Dent Res 2016; 95(12): 1341–1349
34. Goetz SC, Ocbina PJ, Anderson KV. The primary cilium as a Hedgehog signal transduction machine. Methods Cell Biol 2009; 94: 199–222
35. Cai S, Bodle JC, Mathieu PS, Amos A, Hamouda M, Bernacki S, McCarty G, Loboa EG. Primary cilia are sensors of electrical field stimulation to induce osteogenesis of human adipose-derived stem cells. FASEB J 2017; 31(1): 346–355
36. McMurray RJ, Wann AK, Thompson CL, Connelly JT, Knight MM. Surface topography regulates wnt signaling through control of primary cilia structure in mesenchymal stem cells. Sci Rep 2013; 3(1): 3545
37. Yuan X, Cao J, He X, Serra R, Qu J, Cao X, Yang S. Ciliary IFT80 balances canonical versus non-canonical hedgehog signalling for osteoblast differentiation. Nat Commun 2016; 7(1): 11024
38. Huber C, Cormier-Daire V. Ciliary disorder of the skeleton. Am J Med Genet C Semin Med Genet 2012; 160C(3): 165–174
39. Day TF, Yang Y. Wnt and hedgehog signaling pathways in bone development. J Bone Joint Surg Am 2008; 90(Suppl 1): 19–24
40. Rohatgi R, Milenkovic L, Scott MP. Patched1 regulates hedgehog signaling at the primary cilium. Science 2007; 317(5836): 372–376
41. Haycraft CJ, Zhang Q, Song B, Jackson WS, Detloff PJ, Serra R, Yoder BK. Intraflagellar transport is essential for endochondral bone formation. Development 2007; 134(2): 307–316
42. Kikuchi A, Yamamoto H. Tumor formation due to abnormalities in the β-catenin-independent pathway of Wnt signaling. Cancer Sci 2008; 99(2): 202–208
43. Baron R, Kneissel M. WNT signaling in bone homeostasis and disease: from human mutations to treatments. Nat Med 2013; 19(2): 179–192
44. Lancaster MA, Schroth J, Gleeson JG. Subcellular spatial regulation of canonical Wnt signalling at the primary cilium. Nat Cell Biol 2011; 13(6): 700–707
45. Corrigan MA, Ferradaes TM, Riffault M, Hoey DA. Ciliotherapy treatments to enhance biochemically- and biophysically-induced mesenchymal stem cell osteogenesis: a comparison study. Cell Mol Bioeng 2018; 12(1): 53–67
46. Corbit KC, Shyer AE, Dowdle WE, Gaulden J, Singla V, Chen MH, Chuang PT, Reiter JF. Kif3a constrains β-catenin-dependent Wnt signalling through dual ciliary and non-ciliary mechanisms. Nat Cell Biol 2008; 10(1): 70–76
47. Lienkamp S, Ganner A, Walz G. Inversin, Wnt signaling and primary cilia. Differentiation 2012; 83(2): S49–S55
48. Pitaval A, Tseng Q, Bornens M, Théry M. Cell shape and contractility regulate ciliogenesis in cell cycle-arrested cells. J Cell Biol 2010; 191(2): 303–312
49. Li A, Xia X, Yeh J, Kua H, Liu H, Mishina Y, Hao A, Li B. PDGF-AA promotes osteogenic differentiation and migration of mesenchymal stem cell by down-regulating PDGFRα and derepressing BMP-Smad1/5/8 signaling. PLoS One 2014; 9(12): e113785
50. Schmid FM, Schou KB, Vilhelm MJ, Holm MS, Breslin L, Farinelli P, Larsen LA, Andersen JS, Pedersen LB, Christensen ST. IFT20 modulates ciliary PDGFRα signaling by regulating the stability of Cbl E3 ubiquitin ligases. J Cell Biol 2018; 217(1): 151–161
51. Graham S, Leonidou A, Lester M, Heliotis M, Mantalaris A, Tsiridis E. Investigating the role of PDGF as a potential drug therapy in bone formation and fracture healing. Expert Opin Investig Drugs 2009; 18(11): 1633–1654
52. Noda K, Kitami M, Kitami K, Kaku M, Komatsu Y. Canonical and noncanonical intraflagellar transport regulates craniofacial skeletal development. Proc Natl Acad Sci U S A 2016; 113(19): E2589–E2597
53. Schneider L, Clement CA, Teilmann SC, Pazour GJ, Hoffmann EK, Satir P, Christensen ST. PDGFRαα signaling is regulated through the primary cilium in fibroblasts. Curr Biol 2005; 15(20): 1861–1866
54. Umberger NL, Caspary T, Bettencourt-Dias M. Ciliary transport regulates PDGF-AA/αα signaling via elevated mammalian target of rapamycin signaling and diminished PP2A activity. Mol Biol Cell 2015; 26(2): 350–358
55. Poniatowski ŁA, Wojdasiewicz P, Gasik R, Szukiewicz D. Transforming growth factor β family: insight into the role of growth factors in regulation of fracture healing biology and potential clinical applications. Mediators Inflamm 2015; 2015: 137823
56. Anvarian Z, Mykytyn K, Mukhopadhyay S, Pedersen LB, Christensen ST. Cellular signalling by primary cilia in development, organ function and disease. Nat Rev Nephrol 2019; 15(4): 199–219
57. Moore ER, Jacobs CR. The primary cilium as a signaling nexus for growth plate function and subsequent skeletal development. J Orthop Res 2018; 36(2): 533–545
58. Liu M, Alharbi M, Graves D, Yang S. IFT80 is required for fracture healing through controlling the regulation of TGF-β signaling in chondrocyte differentiation and function. J Bone Miner Res 2020; 35(3): 571–582
59. Aspera-Werz RH, Chen T, Ehnert S, Zhu S, Fröhlich T, Nussler AK. Cigarette smoke induces the risk of metabolic bone diseases: transforming growth factor β signaling impairment via dysfunctional primary cilia affects migration, proliferation, and differentiation of human mesenchymal stem cells. Int J Mol Sci 2019; 20(12): 2915
60. Xie YF, Shi WG, Zhou J, Gao YH, Li SF, Fang QQ, Wang MG, Ma HP, Wang JF, Xian CJ, Chen KM. Pulsed electromagnetic fields stimulate osteogenic differentiation and maturation of osteoblasts by upregulating the expression of BMPRII localized at the base of primary cilium. Bone 2016; 93: 22–32
61. Labour MN, Riffault M, Christensen ST, Hoey DA. TGFβ1-induced recruitment of human bone mesenchymal stem cells is mediated by the primary cilium in a SMAD3-dependent manner. Sci Rep 2016; 6(1): 35542
62. Uzbekov RE, Maurel DB, Aveline PC, Pallu S, Benhamou CL, Rochefort GY. Centrosome fine ultrastructure of the osteocyte mechanosensitive primary cilium. Microsc Microanal 2012; 18(6): 1430–1441
63. Sharma D, Ciani C, Marin PA, Levy JD, Doty SB, Fritton SP. Alterations in the osteocyte lacunar-canalicular microenvironment due to estrogen deficiency. Bone 2012; 51(3): 488–497
64. Main RP. Osteocytes and the bone lacunar-canalicular system: insights into bone biology and skeletal function using bone tissue

microstructure. Int J Paleopathol 2017; 18: 44–46
65. Gurkan UA, Akkus O. The mechanical environment of bone marrow: a review. Ann Biomed Eng 2008; 36(12): 1978–1991
66. Whitfield JF. Primary cilium—is it an osteocyte's strain-sensing flowmeter? J Cell Biochem 2003; 89(2): 233–237
67. Pavalko FM, Norvell SM, Burr DB, Turner CH, Duncan RL, Bidwell JP. A model for mechanotransduction in bone cells: the load-bearing mechanosomes. J Cell Biochem 2003; 88(1): 104–112
68. Bonewald LF. Mechanosensation and transduction in osteocytes. Bonekey Osteovision 2006; 3(10): 7–15
69. Stavenschi E, Labour MN, Hoey DA. Oscillatory fluid flow induces the osteogenic lineage commitment of mesenchymal stem cells: the effect of shear stress magnitude, frequency, and duration. J Biomech 2017; 55: 99–106
70. Riddle RC, Taylor AF, Genetos DC, Donahue HJ. MAP kinase and calcium signaling mediate fluid flow-induced human mesenchymal stem cell proliferation. Am J Physiol Cell Physiol 2006; 290(3): C776–C784
71. Metzger TA, Kreipke TC, Vaughan TJ, McNamara LM, Niebur GL. The *in situ* mechanics of trabecular bone marrow: the potential for mechanobiological response. J Biomech Eng 2015; 137(1): 011006
72. Hu K, Sun H, Gui B, Sui C. TRPV4 functions in flow shear stress induced early osteogenic differentiation of human bone marrow mesenchymal stem cells. Biomed Pharmacother 2017; 91: 841–848
73. Yourek G, McCormick SM, Mao JJ, Reilly GC. Shear stress induces osteogenic differentiation of human mesenchymal stem cells. Regen Med 2010; 5(5): 713–724
74. Sonam S, Sathe SR, Yim EK, Sheetz MP, Lim CT. Cell contractility arising from topography and shear flow determines human mesenchymal stem cell fate. Sci Rep 2016; 6(1): 20415
75. Shi W, Zhang Y, Chen K, He J, Feng X, Wei W, Hua J, Wang J. Primary cilia act as microgravity sensors by depolymerizing microtubules to inhibit osteoblastic differentiation and mineralization. Bone 2020; 136: 115346
76. Praetorius HA, Spring KR. Bending the MDCK cell primary cilium increases intracellular calcium. J Membr Biol 2001; 184(1): 71–79
77. Uda Y, Azab E, Sun N, Shi C, Pajevic PD. Osteocyte mechanobiology. Curr Osteoporos Rep 2017; 15(4): 318–325
78. Chen JC, Hoey DA, Chua M, Bellon R, Jacobs CR. Mechanical signals promote osteogenic fate through a primary cilia-mediated mechanism. FASEB J 2016; 30(4): 1504–1511
79. Moore ER, Zhu YX, Ryu HS, Jacobs CR. Periosteal progenitors contribute to load-induced bone formation in adult mice and require primary cilia to sense mechanical stimulation. Stem Cell Res Ther 2018; 9(1): 190
80. Kitase Y, Barragan L, Qing H, Kondoh S, Jiang JX, Johnson ML, Bonewald LF. Mechanical induction of PGE2 in osteocytes blocks glucocorticoid-induced apoptosis through both the β-catenin and PKA pathways. J Bone Miner Res 2010; 25(12): 2657–2668
81. Delaine-Smith RM, Sittichokechaiwut A, Reilly GC. Primary cilia respond to fluid shear stress and mediate flow-induced calcium deposition in osteoblasts. FASEB J 2014; 28(1): 430–439
82. Kaku M, Komatsu Y. Functional diversity of ciliary proteins in bone development and disease. Curr Osteoporos Rep 2017; 15(2): 96–102
83. Liu W, Xu S, Woda C, Kim P, Weinbaum S, Satlin LM. Effect of flow and stretch on the $[Ca^{2+}]i$ response of principal and intercalated cells in cortical collecting duct. Am J Physiol Renal Physiol 2003; 285(5): F998–F1012
84. McGlashan SR, Knight MM, Chowdhury TT, Joshi P, Jensen CG, Kennedy S, Poole CA. Mechanical loading modulates chondrocyte primary cilia incidence and length. Cell Biol Int 2010; 34(5): 441–446
85. Gardner K, Arnoczky SP, Lavagnino M. Effect of *in vitro* stress-deprivation and cyclic loading on the length of tendon cell cilia *in situ*. J Orthop Res 2011; 29(4): 582–587
86. Lin F, Hiesberger T, Cordes K, Sinclair AM, Goldstein LS, Somlo S, Igarashi P. Kidney-specific inactivation of the KIF3A subunit of kinesin-II inhibits renal ciliogenesis and produces polycystic kidney disease. Proc Natl Acad Sci U S A 2003; 100(9): 5286–5291
87. Qiu N, Xiao Z, Cao L, Buechel MM, David V, Roan E, Quarles LD. Disruption of Kif3a in osteoblasts results in defective bone formation and osteopenia. J Cell Sci 2012; 125(8): 1945–1957
88. Kolpakova-Hart E, Jinnin M, Hou B, Fukai N, Olsen BR. Kinesin-2 controls development and patterning of the vertebrate skeleton by Hedgehog- and Gli3-dependent mechanisms. Dev Biol 2007; 309(2): 273–284
89. Temiyasathit S, Tang WJ, Leucht P, Anderson CT, Monica SD, Castillo AB, Helms JA, Stearns T, Jacobs CR. Mechanosensing by the primary cilium: deletion of Kif3A reduces bone formation due to loading. PLoS One 2012; 7(3): e33368
90. Leucht P, Monica SD, Temiyasathit S, Lenton K, Manu A, Longaker MT, Jacobs CR, Spilker RL, Guo H, Brunski JB, Helms JA. Primary cilia act as mechanosensors during bone healing around an implant. Med Eng Phys 2013; 35(3): 392–402
91. Li H. TRP channel classification. Adv Exp Med Biol 2017; 976: 1–8
92. Siroky BJ, Kleene NK, Kleene SJ, Varnell CD Jr, Comer RG, Liu J, Lu L, Pachciarz NW, Bissler JJ, Dixon BP. Primary cilia regulate the osmotic stress response of renal epithelial cells through TRPM3. Am J Physiol Renal Physiol 2017; 312(4): F791–F805
93. Corrigan MA, Johnson GP, Stavenschi E, Riffault M, Labour MN, Hoey DA. TRPV4-mediates oscillatory fluid shear mechanotransduction in mesenchymal stem cells in part via the primary cilium. Sci Rep 2018; 8(1): 3824
94. Mizoguchi F, Mizuno A, Hayata T, Nakashima K, Heller S, Ushida T, Sokabe M, Miyasaka N, Suzuki M, Ezura Y, Noda M. Transient receptor potential vanilloid 4 deficiency suppresses unloading-induced bone loss. J Cell Physiol 2008; 216(1): 47–53
95. Masuyama R, Vriens J, Voets T, Karashima Y, Owsianik G, Vennekens R, Lieben L, Torrekens S, Moermans K, Vanden Bosch A, Bouillon R, Nilius B, Carmeliet G. TRPV4-mediated calcium influx regulates terminal differentiation of osteoclasts. Cell Metab 2008; 8(3): 257–265
96. Winslow MM, Pan M, Starbuck M, Gallo EM, Deng L, Karsenty G, Crabtree GR. Calcineurin/NFAT signaling in osteoblasts regulates bone mass. Dev Cell 2006; 10(6): 771–782
97. Takayanagi H, Kim S, Koga T, Nishina H, Isshiki M, Yoshida H, Saiura A, Isobe M, Yokochi T, Inoue J, Wagner EF, Mak TW,

Kodama T, Taniguchi T. Induction and activation of the transcription factor NFATc1 (NFAT2) integrate RANKL signaling in terminal differentiation of osteoclasts. Dev Cell 2002; 3(6): 889–901

98. O'Conor CJ, Griffin TM, Liedtke W, Guilak F. Increased susceptibility of Trpv4-deficient mice to obesity and obesity-induced osteoarthritis with very high-fat diet. Ann Rheum Dis 2013; 72(2): 300–304
99. Masuyama R, Mizuno A, Komori H, Kajiya H, Uekawa A, Kitaura H, Okabe K, Ohyama K, Komori T. Calcium/calmodulin-signaling supports TRPV4 activation in osteoclasts and regulates bone mass. J Bone Miner Res 2012; 27(8): 1708–1721
100. Lee KL, Guevarra MD, Nguyen AM, Chua MC, Wang Y, Jacobs CR. The primary cilium functions as a mechanical and calcium signaling nexus. Cilia 2015; 4(1): 7
101. Phan MN, Leddy HA, Votta BJ, Kumar S, Levy DS, Lipshutz DB, Lee SH, Liedtke W, Guilak F. Functional characterization of TRPV4 as an osmotically sensitive ion channel in porcine articular chondrocytes. Arthritis Rheum 2009; 60(10): 3028–3037
102. Han SJ, Kim JI, Park KM. P26 Hydrogen sulfide elongates primary cilia in the kidney tubular epithelial cells. Nitric Oxide 2014; 39 (Supplement): S24
103. Miyoshi K, Kasahara K, Miyazaki I, Asanuma M. Factors that influence primary cilium length. Acta Med Okayama 2011; 65(5): 279–285
104. Xiao ZS, Quarles LD. Role of the polycytin-primary cilia complex in bone development and mechanosensing. Ann N Y Acad Sci 2010; 1192(1): 410–421
105. Li Q, Montalbetti N, Wu Y, Ramos A, Raychowdhury MK, Chen XZ, Cantiello HF. Polycystin-2 cation channel function is under the control of microtubular structures in primary cilia of renal epithelial cells. J Biol Chem 2006; 281(49): 37566–37575
106. Nauli SM, Alenghat FJ, Luo Y, Williams E, Vassilev P, Li X, Elia AE, Lu W, Brown EM, Quinn SJ, Ingber DE, Zhou J. Polycystins 1 and 2 mediate mechanosensation in the primary cilium of kidney cells. Nat Genet 2003; 33(2): 129–137
107. Spasic M, Jacobs CR. Primary cilia: cell and molecular mechanosensors directing whole tissue function. Semin Cell Dev Biol 2017; 71: 42–52
108. Qiu N, Cao L, David V, Quarles LD, Xiao Z. Kif3a deficiency reverses the skeletal abnormalities in Pkd1 deficient mice by restoring the balance between osteogenesis and adipogenesis. PLoS One 2010; 5(12): e15240
109. Jin X, Mohieldin AM, Muntean BS, Green JA, Shah JV, Mykytyn K, Nauli SM. Cilioplasm is a cellular compartment for calcium signaling in response to mechanical and chemical stimuli. Cell Mol Life Sci 2014; 71(11): 2165–2178
110. Saunders MM, You J, Zhou Z, Li Z, Yellowley CE, Kunze EL, Jacobs CR, Donahue HJ. Fluid flow-induced prostaglandin E2 response of osteoblastic ROS 17/2.8 cells is gap junction-mediated and independent of cytosolic calcium. Bone 2003; 32(4): 350–356
111. Jing D, Shen G, Huang J, Xie K, Cai J, Xu Q, Wu X, Luo E. Circadian rhythm affects the preventive role of pulsed electromagnetic fields on ovariectomy-induced osteoporosis in rats. Bone 2010; 46(2): 487–495
112. Garland DE, Adkins RH, Matsuno NN, Stewart CA. The effect of pulsed electromagnetic fields on osteoporosis at the knee in individuals with spinal cord injury. J Spinal Cord Med 1999; 22(4): 239–245
113. Tabrah FL, Ross P, Hoffmeier M, Gilbert F Jr. Clinical report on long-term bone density after short-term EMF application. Bioelectromagnetics 1998; 19(2): 75–78
114. Funk RH, Monsees T, Ozkucur N. Electromagnetic effects—from cell biology to medicine. Prog Histochem Cytochem 2009; 43(4): 177–264
115. Yan JL, Zhou J, Ma HP, Ma XN, Gao YH, Shi WG, Fang QQ, Ren Q, Xian CJ, Chen KM. Pulsed electromagnetic fields promote osteoblast mineralization and maturation needing the existence of primary cilia. Mol Cell Endocrinol 2015; 404: 132–140
116. Wang YY, Pu XY, Shi WG, Fang QQ, Chen XR, Xi HR, Gao YH, Zhou J, Xian CJ, Chen KM. Pulsed electromagnetic fields promote bone formation by activating the sAC-cAMP-PKA-CREB signaling pathway. J Cell Physiol 2019; 234(3): 2807–2821
117. Shi W, Gao Y, Wang Y, Zhou J, Wei Z, Ma X, Ma H, Xian CJ, Wang J, Chen K. The flavonol glycoside icariin promotes bone formation in growing rats by activating the cAMP signaling pathway in primary cilia of osteoblasts. J Biol Chem 2017; 292(51): 20883–20896
118. Zhou J, Gao YH, Zhu BY, Shao JL, Ma HP, Xian CJ, Chen KM. Sinusoidal electromagnetic fields increase peak bone mass in rats by activating Wnt10b/-catenin in primary cilia of osteoblasts. J Bone Miner Res 2019; 34(7): 1336–1351
119. McCullen SD, McQuilling JP, Grossfeld RM, Lubischer JL, Clarke LI, Loboa EG. Application of low-frequency alternating current electric fields via interdigitated electrodes: effects on cellular viability, cytoplasmic calcium, and osteogenic differentiation of human adipose-derived stem cells. Tissue Eng Part C Methods 2010; 16(6): 1377–1386
120. Sun S, Liu Y, Lipsky S, Cho M. Physical manipulation of calcium oscillations facilitates osteodifferentiation of human mesenchymal stem cells. FASEB J 2007; 21(7): 1472–1480
121. Khatib L, Golan DE, Cho M. Physiologic electrical stimulation provokes intracellular calcium increase mediated by phospholipase C activation in human osteoblasts. FASEB J 2004; 18(15): 1903–1905
122. Zhang J, Li M, Kang ET, Neoh KG. Electrical stimulation of adipose-derived mesenchymal stem cells in conductive scaffolds and the roles of voltage-gated ion channels. Acta Biomater 2016; 32: 46–56
123. Xu J, Wang W, Clark CC, Brighton CT. Signal transduction in electrically stimulated articular chondrocytes involves translocation of extracellular calcium through voltage-gated channels. Osteoarthritis Cartilage 2009; 17(3): 397–405
124. Bergh JJ, Xu Y, Farach-Carson MC. Osteoprotegerin expression and secretion are regulated by calcium influx through the L-type voltage-sensitive calcium channel. Endocrinology 2004; 145(1): 426–436
125. Reiter JF, Leroux MR. Genes and molecular pathways underpinning ciliopathies. Nat Rev Mol Cell Biol 2017; 18(9): 533–547
126. Novarino G, Akizu N, Gleeson JG. Modeling human disease in humans: the ciliopathies. Cell 2011; 147(1): 70–79
127. Wheway G, Parry DA, Johnson CA. The role of primary cilia in the development and disease of the retina. Organogenesis 2014; 10(1): 69–85

128. Waters AM, Beales PL. Ciliopathies: an expanding disease spectrum. Pediatr Nephrol 2011; 26(7): 1039–1056
129. Perrault I, Saunier S, Hanein S, Filhol E, Bizet AA, Collins F, Salih MA, Gerber S, Delphin N, Bigot K, Orssaud C, Silva E, Baudouin V, Oud MM, Shannon N, Le Merrer M, Roche O, Pietrement C, Goumid J, Baumann C, Bole-Feysot C, Nitschke P, Zahrate M, Beales P, Arts HH, Munnich A, Kaplan J, Antignac C, Cormier-Daire V, Rozet JM. Mainzer-Saldino syndrome is a ciliopathy caused by IFT140 mutations. Am J Hum Genet 2012; 90(5): 864–870
130. Rix S, Calmont A, Scambler PJ, Beales PL. An Ift80 mouse model of short rib polydactyly syndromes shows defects in hedgehog signalling without loss or malformation of cilia. Hum Mol Genet 2011; 20(7): 1306–1314
131. Dagoneau N, Goulet M, Geneviève D, Sznajer Y, Martinovic J, Smithson S, Huber C, Baujat G, Flori E, Tecco L, Cavalcanti D, Delezoide AL, Serre V, Le Merrer M, Munnich A, Cormier-Daire V. DYNC2H1 mutations cause asphyxiating thoracic dystrophy and short rib-polydactyly syndrome, type III. Am J Hum Genet 2009; 84(5): 706–711
132. Saldino RM, Noonan CD. Severe thoracic dystrophy with striking micromelia, abnormal osseous development, including the spine, and multiple visceral anomalies. Am J Roentgenol Radium Ther Nucl Med 1972; 114(2): 257–263
133. Yang SS, Roth JA, Langer LO Jr. Short rib syndrome Beemer-Langer type with polydactyly: a multiple congenital anomalies syndrome. Am J Med Genet 1991; 39(3): 243–246
134. Elçioglu NH, Hall CM. Diagnostic dilemmas in the short rib-polydactyly syndrome group. Am J Med Genet 2002; 111(4): 392–400
135. Majewski F, Pfeiffer RA, Lenz W, Müller R, Feil G, Seiler R. Polysyndactyly, short limbs, and genital malformations—a new syndrome? Z Kinderheilkd 1971; 111(2): 118–138 (in German)
136. Naumoff P, Young LW, Mazer J, Amortegui AJ. Short rib-polydactyly syndrome type 3. Radiology 1977; 122(2): 443–447
137. Meizner I, Barnhard Y. Short-rib polydactyly syndrome (SRPS) type III diagnosed during routine prenatal ultrasonographic screening. A case report. Prenat Diagn 1995; 15(7): 665–668
138. Cideciyan D, Rodriguez MM, Haun RL, Abdenour GE, Bruce JH. New findings in short rib syndrome. Am J Med Genet 1993; 46(3): 255–259
139. Schmidts M, Arts HH, Bongers EMHF, Yap Z, Oud MM, Antony D, Duijkers L, Emes RD, Stalker J, Yntema JBL, Plagnol V, Hoischen A, Gilissen C, Forsythe E, Lausch E, Veltman JA, Roeleveld N, Superti-Furga A, Kutkowska-Kazmierczak A, Kamsteeg EJ, Elçioğlu N, van Maarle MC, Graul-Neumann LM, Devriendt K, Smithson SF, Wellesley D, Verbeek NE, Hennekam RCM, Kayserili H, Scambler PJ, Beales PL; UK10K, Knoers NV, Roepman R, Mitchison HM. Exome sequencing identifies DYNC2H1 mutations as a common cause of asphyxiating thoracic dystrophy (Jeune syndrome) without major polydactyly, renal or retinal involvement. J Med Genet 2013; 50(5): 309–323
140. Baujat G, Huber C, El Hokayem J, Caumes R, Do Ngoc Thanh C, David A, Delezoide AL, Dieux-Coeslier A, Estournet B, Francannet C, Kayirangwa H, Lacaille F, Le Bourgeois M, Martinovic J, Salomon R, Sigaudy S, Malan V, Munnich A, Le Merrer M, Le Quan Sang KH, Cormier-Daire V. Asphyxiating thoracic dysplasia: clinical and molecular review of 39 families. J Med Genet 2013; 50(2): 91–98
141. Schmidts M, Frank V, Eisenberger T, Al Turki S, Bizet AA, Antony D, Rix S, Decker C, Bachmann N, Bald M, Vinke T, Toenshoff B, Di Donato N, Neuhann T, Hartley JL, Maher ER, Bogdanović R, Peco-Antić A, Mache C, Hurles ME, Joksić I, Guć-Šćekić M, Dobricic J, Brankovic-Magic M, Bolz HJ, Pazour GJ, Beales PL, Scambler PJ, Saunier S, Mitchison HM, Bergmann C. Combined NGS approaches identify mutations in the intraflagellar transport gene IFT140 in skeletal ciliopathies with early progressive kidney disease. Hum Mutat 2013; 34(5): 714–724
142. Tüysüz B, Bariş S, Aksoy F, Madazli R, Ungür S, Sever L. Clinical variability of asphyxiating thoracic dystrophy (Jeune) syndrome: Evaluation and classification of 13 patients. Am J Med Genet A 2009; 149A(8): 1727–1733
143. Jonassen JA, SanAgustin J, Baker SP, Pazour GJ. Disruption of IFT complex A causes cystic kidneys without mitotic spindle misorientation. J Am Soc Nephrol 2012; 23(4): 641–651
144. Schmidts M, Vodopiutz J, Christou-Savina S, Cortés CR, McInerney-Leo AM, Emes RD, Arts HH, Tüysüz B, D'Silva J, Leo PJ, Giles TC, Oud MM, Harris JA, Koopmans M, Marshall M, Elçioglu N, Kuechler A, Bockenhauer D, Moore AT, Wilson LC, Janecke AR, Hurles ME, Emmet W, Gardiner B, Streubel B, Dopita B, Zankl A, Kayserili H, Scambler PJ, Brown MA, Beales PL, Wicking C; UK10K, Duncan EL, Mitchison HM. Mutations in the gene encoding IFT dynein complex component WDR34 cause Jeune asphyxiating thoracic dystrophy. Am J Hum Genet 2013; 93(5): 932–944
145. Oberklaid F, Danks DM, Mayne V, Campbell P. Asphyxiating thoracic dysplasia. Clinical, radiological, and pathological information on 10 patients. Arch Dis Child 1977; 52(10): 758–765
146. Beals RK, Weleber RG. Conorenal dysplasia: a syndrome of cone-shaped epiphysis, renal disease in childhood, retinitis pigmentosa and abnormality of the proximal femur. Am J Med Genet A 2007; 143A(20): 2444–2447
147. Eke T, Woodruff G, Young ID. A new oculorenal syndrome: retinal dystrophy and tubulointerstitial nephropathy in cranioectodermal dysplasia. Br J Ophthalmol 1996; 80(5): 490–491
148. Walczak-Sztulpa J, Eggenschwiler J, Osborn D, Brown DA, Emma F, Klingenberg C, Hennekam RC, Torre G, Garshasbi M, Tzschach A, Szczepanska M, Krawczynski M, Zachwieja J, Zwolinska D, Beales PL, Ropers HH, Latos-Bielenska A, Kuss AW. Cranioectodermal dysplasia, Sensenbrenner syndrome, is a ciliopathy caused by mutations in the IFT122 gene. Am J Hum Genet 2010; 86(6): 949–956
149. Bredrup C, Saunier S, Oud MM, Fiskerstrand T, Hoischen A, Brackman D, Leh SM, Midtbø M, Filhol E, Bole-Feysot C, Nitschké P, Gilissen C, Haugen OH, Sanders JS, Stolte-Dijkstra I, Mans DA, Steenbergen EJ, Hamel BC, Matignon M, Pfundt R, Jeanpierre C, Boman H, Rødahl E, Veltman JA, Knappskog PM, Knoers NV, Roepman R, Arts HH. Ciliopathies with skeletal anomalies and renal insufficiency due to mutations in the IFT-A gene WDR19. Am J Hum Genet 2011; 89(5): 634–643
150. Lee E, Sivan-Loukianova E, Eberl DF, Kernan MJ. An IFT-A protein is required to delimit functionally distinct zones in mechanosensory cilia. Curr Biol 2008; 18(24): 1899–1906
151. Merrill AE, Merriman B, Farrington-Rock C, Camacho N, Sebald

ET, Funari VA, Schibler MJ, Firestein MH, Cohn ZA, Priore MA, Thompson AK, Rimoin DL, Nelson SF, Cohn DH, Krakow D. Ciliary abnormalities due to defects in the retrograde transport protein DYNC2H1 in short-rib polydactyly syndrome. Am J Hum Genet 2009; 84(4): 542–549

152. Porter ME, Bower R, Knott JA, Byrd P, Dentler W. Cytoplasmic dynein heavy chain 1b is required for flagellar assembly in *Chlamydomonas*. Mol Biol Cell 1999; 10(3): 693–712
153. Miller KA, Ah-Cann CJ, Welfare MF, Tan TY, Pope K, Caruana G, Freckmann ML, Savarirayan R, Bertram JF, Dobbie MS, Bateman JF, Farlie PG. Cauli: a mouse strain with an Ift140 mutation that results in a skeletal ciliopathy modelling Jeune syndrome. PLoS Genet 2013; 9(8): e1003746
154. Beales PL, Bland E, Tobin JL, Bacchelli C, Tuysuz B, Hill J, Rix S, Pearson CG, Kai M, Hartley J, Johnson C, Irving M, Elcioglu N, Winey M, Tada M, Scambler PJ. IFT80, which encodes a conserved intraflagellar transport protein, is mutated in Jeune asphyxiating thoracic dystrophy. Nat Genet 2007; 39(6): 727–729
155. Davis EE, Zhang Q, Liu Q, Diplas BH, Davey LM, Hartley J, Stoetzel C, Szymanska K, Ramaswami G, Logan CV, Muzny DM, Young AC, Wheeler DA, Cruz P, Morgan M, Lewis LR, Cherukuri P, Maskeri B, Hansen NF, Mullikin JC, Blakesley RW, Bouffard GG; NISC Comparative Sequencing Program,Gyapay G, Rieger S, Tönshoff B, Kern I, Soliman NA, Neuhaus TJ, Swoboda KJ, Kayserili H, Gallagher TE, Lewis RA, Bergmann C, Otto EA, Saunier S, Scambler PJ, Beales PL, Gleeson JG, Maher ER, Attié-Bitach T, Dollfus H, Johnson CA, Green ED, Gibbs RA, Hildebrandt F, Pierce EA, Katsanis N, Katsanis N. TTC21B contributes both causal and modifying alleles across the ciliopathy spectrum. Nat Genet 2011; 43(3): 189–196
156. Halbritter J, Bizet AA, Schmidts M, Porath JD, Braun DA, Gee HY, McInerney-Leo AM, Krug P, Filhol E, Davis EE, Airik R, Czarnecki PG, Lehman AM, Trnka P, Nitschké P, Bole-Feysot C, Schueler M, Knebelmann B, Burtey S, Szabó AJ, Tory K, Leo PJ, Gardiner B, McKenzie FA, Zankl A, Brown MA, Hartley JL, Maher ER, Li C, Leroux MR, Scambler PJ, Zhan SH, Jones SJ, Kayserili H, Tuysuz B, Moorani KN, Constantinescu A, Krantz ID, Kaplan BS, Shah JV; UK10K Consortium,Hurd TW, Doherty D, Katsanis N, Duncan EL, Otto EA, Beales PL, Mitchison HM, Saunier S, Hildebrandt F. Defects in the IFT-B component IFT172 cause Jeune and Mainzer-Saldino syndromes in humans. Am J Hum Genet 2013; 93(5): 915–925
157. Tao D, Xue H, Zhang C, Li G, Sun Y. The role of IFT140 in osteogenesis of adult mice long bone. J Histochem Cytochem 2019; 67(8): 601–611
158. Gao D, Wang R, Li B, Yang Y, Zhai Z, Chen DY. WDR34 is a novel TAK1-associated suppressor of the IL-1R/TLR3/TLR4-induced NF-κB activation pathway. Cell Mol Life Sci 2009; 66(15): 2573–2584
159. Krock BL, Mills-Henry I, Perkins BD. Retrograde intraflagellar transport by cytoplasmic dynein-2 is required for outer segment extension in vertebrate photoreceptors but not arrestin translocation. Invest Ophthalmol Vis Sci 2009; 50(11): 5463–5471
160. Ruiz-Perez VL, Blair HJ, Rodriguez-Andres ME, Blanco MJ, Wilson A, Liu YN, Miles C, Peters H, Goodship JA. Evc is a positive mediator of Ihh-regulated bone growth that localises at the base of chondrocyte cilia. Development 2007; 134(16): 2903–2912
161. Caparrós-Martín JA, Valencia M, Reytor E, Pacheco M, Fernandez M, Perez-Aytes A, Gean E, Lapunzina P, Peters H, Goodship JA, Ruiz-Perez VL. The ciliary Evc/Evc2 complex interacts with Smo and controls Hedgehog pathway activity in chondrocytes by regulating Sufu/Gli3 dissociation and Gli3 trafficking in primary cilia. Hum Mol Genet 2013; 22(1): 124–139
162. Martik ML, Bronner ME. Regulatory logic underlying diversification of the neural crest. Trends Genet 2017; 33(10): 715–727
163. Cortés CR, Metzis V, Wicking C. Unmasking the ciliopathies: craniofacial defects and the primary cilium. Wiley Interdiscip Rev Dev Biol 2015; 4(6): 637–653
164. Wang SF, Kowal TJ, Ning K, Koo EB, Wu AY, Mahajan VB, Sun Y. Review of ocular manifestations of Joubert syndrome. Genes (Basel) 2018; 9(12): 605
165. Molinari E, Ramsbottom SA, Srivastava S, Booth P, Alkanderi S, McLafferty SM, Devlin LA, White K, Gunay-Aygun M, Miles CG, Sayer JA. Targeted exon skipping rescues ciliary protein composition defects in Joubert syndrome patient fibroblasts. Sci Rep 2019; 9(1): 10828
166. Del Giudice E, Macca M, Imperati F, D'Amico A, Parent P, Pasquier L, Layet V, Lyonnet S, Stamboul-Darmency V, Thauvin-Robinet C, Franco B; Oral-Facial-Digital Type I (OFD1) Collaborative Group. CNS involvement in OFD1 syndrome: a clinical, molecular, and neuroimaging study. Orphanet J Rare Dis 2014; 9(1): 74
167. Singla V, Romaguera-Ros M, Garcia-Verdugo JM, Reiter JF. Ofd1, a human disease gene, regulates the length and distal structure of centrioles. Dev Cell 2010; 18(3): 410–424
168. Ferrante MI, Giorgio G, Feather SA, Bulfone A, Wright V, Ghiani M, Selicorni A, Gammaro L, Scolari F, Woolf AS, Sylvie O, Bernard L, Malcolm S, Winter R, Ballabio A, Franco B. Identification of the gene for oral-facial-digital type I syndrome. Am J Hum Genet 2001; 68(3): 569–576
169. AlKattan WM, Al-Qattan MM, Bafaqeeh SA. The pathogenesis of the clinical features of oral-facial-digital syndrome type I. Saudi Med J 2015; 36(11): 1277–1284
170. Ferrante MI, Zullo A, Barra A, Bimonte S, Messaddeq N, Studer M, Dollé P, Franco B. Oral-facial-digital type I protein is required for primary cilia formation and left-right axis specification. Nat Genet 2006; 38(1): 112–117
171. Romani M, Mancini F, Micalizzi A, Poretti A, Miccinilli E, Accorsi P, Avola E, Bertini E, Borgatti R, Romaniello R, Ceylaner S, Coppola G, D'Arrigo S, Giordano L, Janecke AR, Lituania M, Ludwig K, Martorell L, Mazza T, Odent S, Pinelli L, Poo P, Santucci M, Signorini S, Simonati A, Spiegel R, Stanzial F, Steinlin M, Tabarki B, Wolf NI, Zibordi F, Boltshauser E, Valente EM. Oral-facial-digital syndrome type VI: is C5orf42 really the major gene? Hum Genet 2015; 134(1): 123–126
172. Poretti A, Vitiello G, Hennekam RC, Arrigoni F, Bertini E, Borgatti R, Brancati F, D'Arrigo S, Faravelli F, Giordano L, Huisman TA, Iannicelli M, Kluger G, Kyllerman M, Landgren M, Lees MM, Pinelli L, Romaniello R, Scheer I, Schwarz CE, Spiegel R, Tibussek D, Valente EM, Boltshauser E. Delineation and diagnostic criteria of oral-facial-digital syndrome type VI. Orphanet J Rare Dis 2012; 7(1): 4
173. Asadollahi R, Strauss JE, Zenker M, Beuing O, Edvardson S,

Elpeleg O, Strom TM, Joset P, Niedrist D, Otte C, Oneda B, Boonsawat P, Azzarello-Burri S, Bartholdi D, Papik M, Zweier M, Haas C, Ekici AB, Baumer A, Boltshauser E, Steindl K, Nothnagel M, Schinzel A, Stoeckli ET, Rauch A. Clinical and experimental evidence suggest a link between KIF7 and C5orf42-related ciliopathies through Sonic Hedgehog signaling. Eur J Hum Genet 2018; 26(2): 197–209

174. Tobin JL, Di Franco M, Eichers E, May-Simera H, Garcia M, Yan J, Quinlan R, Justice MJ, Hennekam RC, Briscoe J, Tada M, Mayor R, Burns AJ, Lupski JR, Hammond P, Beales PL. Inhibition of neural crest migration underlies craniofacial dysmorphology and Hirschsprung's disease in Bardet–Biedl syndrome. Proc Natl Acad Sci U S A 2008; 105(18): 6714–6719
175. Borgström MK, Riise R, Tornqvist K, Granath L. Anomalies in the permanent dentition and other oral findings in 29 individuals with Laurence–Moon–Bardet–Biedl syndrome. J Oral Pathol Med 1996; 25(2): 86–89
176. Beales PL, Elcioglu N, Woolf AS, Parker D, Flinter FA. New criteria for improved diagnosis of Bardet–Biedl syndrome: results of a population survey. J Med Genet 1999; 36(6): 437–446
177. Andersson EM, Axelsson S, Gjølstad LF, Storhaug K. Taurodontism: a minor diagnostic criterion in Laurence–Moon/Bardet–Biedl syndromes. Acta Odontol Scand 2013; 71(6): 1671–1674
178. Heon E, Kim G, Qin S, Garrison JE, Tavares E, Vincent A, Nuangchamnong N, Scott CA, Slusarski DC, Sheffield VC. Mutations in C8ORF37 cause Bardet Biedl syndrome (BBS21). Hum Mol Genet 2016; 25(11): 2283–2294
179. Ludlam WG, Aoba T, Cuéllar J, Bueno-Carrasco MT, Makaju A, Moody JD, Franklin S, Valpuesta JM, Willardson BM. Molecular architecture of the Bardet-Biedl syndrome protein 2-7-9 subcomplex. J Biol Chem 2019; 294(44): 16385–16399
180. Tayeh MK, Yen HJ, Beck JS, Searby CC, Westfall TA, Griesbach H, Sheffield VC, Slusarski DC. Genetic interaction between Bardet–Biedl syndrome genes and implications for limb patterning. Hum Mol Genet 2008; 17(13): 1956–1967
181. Zhang Q, Seo S, Bugge K, Stone EM, Sheffield VC. BBS proteins interact genetically with the IFT pathway to influence SHH-related phenotypes. Hum Mol Genet 2012; 21(9): 1945–1953
182. Valencia M, Lapunzina P, Lim D, Zannolli R, Bartholdi D, Wollnik B, Al-Ajlouni O, Eid SS, Cox H, Buoni S, Hayek J, Martinez-Frias ML, Antonio PA, Temtamy S, Aglan M, Goodship JA, Ruiz-Perez VL. Widening the mutation spectrum of EVC and EVC2: ectopic expression of Weyer variants in NIH 3T3 fibroblasts disrupts Hedgehog signaling. Hum Mutat 2009; 30(12): 1667–1675
183. Shen W, Han D, Zhang J, Zhao H, Feng H. Two novel heterozygous mutations of EVC2 cause a mild phenotype of Ellis-van Creveld syndrome in a Chinese family. Am J Med Genet Part A 2011; 155 (9): 2131–2136
184. Ruiz-Perez VL, Ide SE, Strom TM, Lorenz B, Wilson D, Woods K, King L, Francomano C, Freisinger P, Spranger S, Marino B, Dallapiccola B, Wright M, Meitinger T, Polymeropoulos MH, Goodship J. Mutations in a new gene in Ellis-van Creveld syndrome and Weyers acrodental dysostosis. Nat Genet 2000; 24(3): 283–286
185. Baujat G, Le Merrer M. Ellis-van Creveld syndrome. Orphanet J Rare Dis 2007; 2(1): 27
186. Hampl M, Cela P, Szabo-Rogers HL, Kunova Bosakova M, Dosedelova H, Krejci P, Buchtova M. Role of primary cilia in odontogenesis. J Dent Res 2017; 96(9): 965–974
187. Nakatomi M, Hovorakova M, Gritli-Linde A, Blair HJ, MacArthur K, Peterka M, Lesot H, Peterkova R, Ruiz-Perez VL, Goodship JA, Peters H. Evc regulates a symmetrical response to Shh signaling in molar development. J Dent Res 2013; 92(3): 222–228
188. Curry CJ, Hall BD. Polydactyly, conical teeth, nail dysplasia, and short limbs: a new autosomal dominant malformation syndrome. Birth Defects Orig Artic Ser 1979; 15(5B): 253–263
189. Roubicek M, Spranger J. Weyers acrodental dysostosis in a family. Clin Genet 1984; 26(6): 587–590
190. Ye X, Song G, Fan M, Shi L, Jabs EW, Huang S, Guo R, Bian Z. A novel heterozygous deletion in the EVC2 gene causes Weyers acrofacial dysostosis. Hum Genet 2006; 119(1-2): 199–205
191. Veis A. Mineral-matrix interactions in bone and dentin. J Bone Miner Res 1993; 8(Suppl 2): S493–S497
192. Hisamoto M, Goto M, Muto M, Nio-Kobayashi J, Iwanaga T, Yokoyama A. Developmental changes in primary cilia in the mouse tooth germ and oral cavity. Biomed Res 2016; 37(3): 207–214
193. Kero D, Novakovic J, Vukojevic K, Petricevic J, Kalibovic Govorko D, Biocina-Lukenda D, Saraga-Babic M. Expression of Ki-67, Oct-4, γ-tubulin and α-tubulin in human tooth development. Arch Oral Biol 2014; 59(11): 1119–1129
194. Jung SY, Green DW, Jung HS, Kim EJ. Cell cycle of the enamel knot during tooth morphogenesis. Histochem Cell Biol 2018; 149(6): 655–659
195. Jernvall J, Kettunen P, Karavanova I, Martin LB, Thesleff I. Evidence for the role of the enamel knot as a control center in mammalian tooth cusp formation: non-dividing cells express growth stimulating Fgf-4 gene. Int J Dev Biol 1994; 38(3): 463–469
196. Thivichon-Prince B, Couble ML, Giamarchi A, Delmas P, Franco B, Romio L, Struys T, Lambrichts I, Ressnikoff D, Magloire H, Bleicher F. Primary cilia of odontoblasts: possible role in molar morphogenesis. J Dent Res 2009; 88(10): 910–915
197. Yuan X, Liu M, Cao X, Yang S. Ciliary IFT80 regulates dental pulp stem cells differentiation by FGF/FGFR1 and Hh/BMP2 signaling. Int J Biol Sci 2019; 15(10): 2087–2099
198. Dassule HR, Lewis P, Bei M, Maas R, McMahon AP. Sonic hedgehog regulates growth and morphogenesis of the tooth. Development 2000; 127(22): 4775–4785
199. Ohazama A, Haycraft CJ, Seppala M, Blackburn J, Ghafoor S, Cobourne M, Martinelli DC, Fan CM, Peterkova R, Lesot H, Yoder BK, Sharpe PT. Primary cilia regulate Shh activity in the control of molar tooth number. Development 2009; 136(6): 897–903
200. Liu B, Chen S, Cheng D, Jing W, Helms JA. Primary cilia integrate hedgehog and Wnt signaling during tooth development. J Dent Res 2014; 93(5): 475–482
201. Li G, Liu M, Zhang S, Wan H, Zhang Q, Yue R, Yan X, Wang X, Wang Z, Sun Y. Essential role of IFT140 in promoting dentinogenesis. J Dent Res 2018; 97(4): 423–431
202. Li X, Yang S, Han L, Mao K, Yang S. Ciliary IFT80 is essential for intervertebral disc development and maintenance. FASEB J 2020; 34(5): 6741–6756
203. Kitamura A, Kawasaki M, Kawasaki K, Meguro F, Yamada A, Nagai T, Kodama Y, Trakanant S, Sharpe PT, Maeda T, Takagi R, Ohazama A. Ift88 is involved in mandibular development. J Anat 2020; 236(2): 317–324